Regions of JFH-1 essential for replication. In order to determine which regions of JFH-1 are important for JFH-1 RNA replication, we constructed a series of chimeric JFH-1 subgenomic replicons replacing the 5'UTR, NS3, NS4AB, NS5A, and NS5B-to-3'X (N5BX) regions from the J6CF strain and tested their replication abilities. For this analysis, we adopted luciferase replicon systems (20) because colony formation assays are time-consuming to perform and it is difficult to evaluate precise replication levels using this method. Furthermore, efficient JFH-1 RNA replication may reduce cellular growth, thus affecting colony formation efficiency (34). We constructed JFH-1 chimeric subgenomic luciferase replicons with the J6CF clone because this clone was reportedly infectious in a chimpanzee (49). However, the JCH-1 and JCH-4 clones were not tested for infectivity. The 5'UTR, NS3, NS4AB, NS5A, or N5BX sequences of the JFH-1 replicon were replaced by J6CF sequences (5'UTR-J6, NS3-J6, NS4-J6, NS5A-J6, or N5BX-J6, respectively [Fig. 2A]). The luciferase activities of these replicons are shown in Fig. 2B. The JFH-1 subgenomic replicon replicated efficiently and had a luciferase activity of approximately 10^7 RLU (Fig. 2B, JFH-1 wt). GND, which was replication incompetent because of a mutation at the GDD motif in the NS5B region, had a luciferase activity of only 10^3 RLU (Fig. 2B, JFH-1/GND), which was taken as the background level. The J6CF subgenomic replicon did not replicate and had the same luciferase activity as GND (Fig. 2B, J6CF wt). Replacement of the 5'UTR, NS4AB, and NS5A sequences of JFH-1 by J6CF sequences (5'UTR-J6, NS4-J6, and NS5A-J6, respectively) did not reduce replication (Fig. 2B, 5'UTR-J6 and NS4-J6) or reduced it only slightly (Fig. 2B, NS5A-J6). However, there was no replication for the JFH-1 chimera with J6 N5BX (Fig. 2B, N5BX-J6). In addition, the JFH-1 chimera with the J6 NS3 region (NS3-J6) had a replication level that was more than 10-fold lower at 24 h and around 10-fold lower at 48 h than that of the wild-type JFH-1 replicon (Fig. 2B, JFH-1 wt and NS3-J6). These data show that the JFH-1 NS5B-to-3'X region is essential for JFH-1 RNA replication and indicate that the JFH-1 NS3 region is also important for JFH-1 RNA replication.

Involvement of the NS3 helicase region in efficient JFH-1 replication. The JFH-1 chimera with the J6 NS3 region (NS3-J6) reduced the replication level (Fig. 2B, NS3-J6). The NS3 protein is known to have two domains: a protease domain at the amino terminal one-third and a helicase domain at the carboxyl terminal two-thirds. To determine which region is important for replication, we compared the replication activity of a JFH-1 chimera with that of the NS3 protease-coding region of J6CF (N3P-J6) and that of a JFH-1 chimera with that of the NS3 helicase-coding region of J6CF (N3H-J6) (Fig. 2A, JFH-1/N3P-J6 and JFH-1/N3H-J6). Although N3P-J6 had the same luciferase activity as JFH-1, N3H-J6 had lower activity than JFH-1 (Fig. 2B, N3P-J6 and N3H-J6). These data show that the JFH-1 NS3 helicase-coding region has an important role in JFH-1 replication.

Importance of the JFH-1 NS5B-coding region and 3'UTR in replication. The JFH-1 chimera with J6 N5BX completely abolished replicon replication (Fig. 2B, N5BX-J6). The N5BX region contains two regions, the NS5B protein-coding region and the 3'UTR. The NS5B protein-coding region encodes RNA-dependent RNA polymerase. To analyze which region of N5BX is important for replication, we separated N5BX into two regions, that is, the NS5B-coding region and the 3'UTR. JFH-1 replicons with NS5B or with the 3'UTR of J6 were constructed (Fig. 2A, JFH-1/N5B-J6 and JFH-1/3'UTR-J6) and their replication abilities analyzed. The replication level of JFH-1/N5B-J6 was reduced more than 100-fold compared with that of the wild-type JFH-1 replicon at 48 h (Fig. 2B, N5B-J6). JFH-1/3'UTR-J6 replicated similarly to JFH-1 at 48 h, but the replication activity at 24 h was reduced more than 10-fold compared with that of the original JFH-1 replicon (Fig. 2B, 3'UTR-J6). These data indicate that the NS5B-coding region and the 3'UTR of JFH-1 are both involved in efficient JFH-1 replication.

Rescue of J6CF replicon replication by incorporation of the JFH-1 sequences. Because the JFH-1 N5BX region appeared to be essential for JFH-1 replication (Fig. 2B, N5BX-J6), we tested whether JFH-1 N5BX could restore the replication of J6CF RNA. We constructed a chimeric J6CF subgenomic replicon containing the JFH-1 N5BX region (Fig. 3A, J6/N5BX-JFH1) and tested its replication abilities. The luciferase activity of J6CF subgenomic RNA was recovered by inclusion of JFH-1 N5BX (Fig. 3B, N5BX-JFH1), but this chimeric replicon showed lower replication activity than the original JFH-1 replicon (Fig. 3B, JFH-1 wt). Furthermore, J6CF replication was not restored by only JFH-1 NS5B (J6/N5B-JFH1) or only the 3'UTR (J6/3'UTR-JFH1) (Fig. 3B, N5B-JFH1 or 3'UTR-JFH1, respectively). These observations clearly indicate that the JFH-1 NS5B-to-3'X region is essential, and the NS5B-coding region and 3'UTR are both important for efficient RNA replication in Huh7 cells. However, other JFH-1 regions are also involved in efficient replication.

The JFH-1 NS3 helicase-coding region was also important for efficient replication, and we thus tested whether the JFH-1 NS3 helicase region by itself could restore J6CF replication (as occurred for the JFH-1 N5BX region). Insertion of only the NS3 helicase region of JFH-1 into J6CF (Fig. 3A, J6/N3H-JFH1) did not restore replication (Fig. 3B, N3H-JFH1). However, replication of the J6 chimeric replicon seemed considerably restored by insertion of JFH-1 NS5B or the 3'UTR in addition to the NS3 helicase-coding region (Fig. 3B, N3H+N5B-JFH-1 or N3H+3'UTR-JFH-1, respectively) and fully restored by insertion of the JFH-1 NS3 helicase region and JFH-1 N5BX region (Fig. 3B, N3H+N5BX-JFH1). These results indicate that the JFH-1 N5BX region is essential for subgenomic-replicon replication and that the JFH-1 NS3 helicase-coding region has an additional role in replication. This was also confirmed by analysis of the replication abilities of JFH-1 replicons with double substitutions of J6CF (Fig. 2A, JFH-1/N3H+N5B-J6, JFH-1/N3H+3'UTR-J6, and JFH-1/N3H+N5BX-J6). Neither of these chimeric JFH-1 replicons replicated (Fig. 2B, N3H+N5B-J6, N3H+3'UTR-J6, and N3H+N5BX-J6).

The NS3 helicase and NS5B-3'X regions of JFH-1 can restore the replication of other genotype 2a replicons but not of genotype 1 replicons. To test whether the JFH-1 NS3 helicase and N5BX regions could restore other HCV replicon replication, chimeric replicon constructs N3H-JFH1, N5BX-JFH1, and N3H+N5BX-JFH1 were constructed using two genotype 2a replicons (JCH-1 and JCH-4), a genotype 1a replicon (H77c), and a genotype 1b replicon (Con1), respectively. The

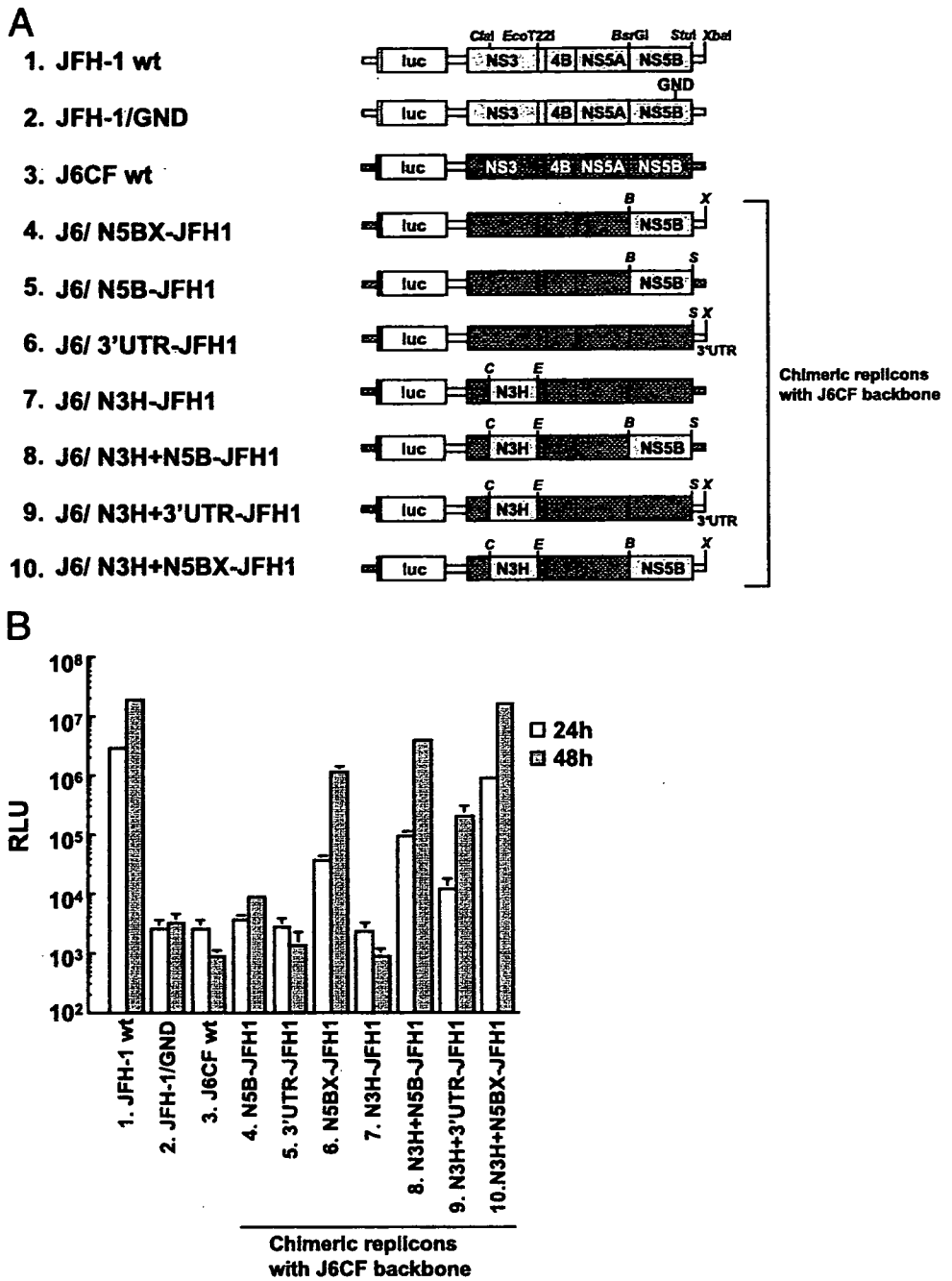

FIG. 3. Luciferase activities of chimeric replicons with a J6CF backbone. (A) Structures of chimeric subgenomic replicons with a J6CF backbone. The restriction enzyme recognition sites used for the construction of plasmids are indicated. *C*, ClaI; *E*, EcoT22I; *B*, BsrGI; *S*, StuI; *X*, XbaI; wt, wild type. (B) Wild-type or chimeric subgenomic RNAs were transfected into Huh7 cells, and the luciferase activities of the transfected cells were examined as described in the legend to Fig. 2B. Assays were performed three times independently, and data are presented as means and standard deviations for luciferase activity (RLU) at 24 h (white bars) and 48 h (gray bars) after transfection.

replication level of each wild-type and chimeric replicon was evaluated by luciferase activity measurement after transient transfection of replicon RNA. No replication of any of the wild-type replicons (Fig. 4, JCH-1 wt, JCH-4 wt, H77c wt, and Con1 wt) or of any of the replicons with insertion of the JFH-1 NS3 helicase region (Fig. 4, JCH-1/N3H-JFH1, JCH-4/N3H-JFH1, H77c/N3H-JFH1, and Con1/N3H-JFH1) was detected. However, genotype 2a replicons with insertion of the JFH-1 N5BX region increased their replication levels severalfold at 48 h (Fig. 4, JCH-1/N5BX-JFH1 and JCH-4/N5BX-JFH1). Furthermore, insertion of both the N3H and the N5BX regions increased the JCH-1 replication over 10-fold compared to that

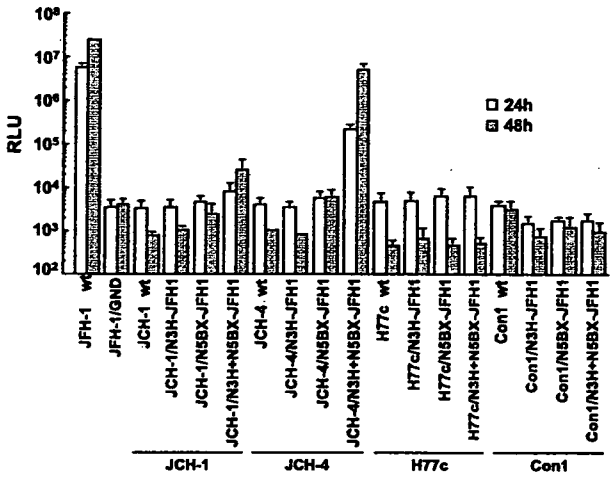

FIG. 4. Restoration of genotype 2a and genotype 1 replicon replication by the insertion of JFH-1 sequences. Two genotype 2a replicons, JCH-1 and JCH-4, a genotype 1a replicon, H77c, and a genotype 1b replicon, Con-1, were used in this assay. Three kinds of chimeric replicons, N3H-JFH-1, N5BX-JFH1, and N3H+N5BX-JFH-1, were prepared for all four HCV replicons. Wild-type (wt) or chimeric subgenomic RNAs were transfected into Huh7 cells and the luciferase activities of the transfected cells examined as described in the legend to Fig. 2B. The assays were performed three times independently, and data are presented as means and standard deviations for luciferase activity (RLU) at 24 h (white bars) and 48 h (gray bars) after transfection.

of wild-type JCH-1 at 48 h and recovered the JCH-4 replication to a level similar to that of wild-type JFH-1 at 48 h (Fig. 4, JCH-1/N3H+N5BX-JFH1 and JCH-4/N3H+N5BX-JFH1, respectively). On the other hand, insertion of the JFH-1 N5BX region or both the N3H and the N5BX regions did not restore H77c or Con1 replicon replication (Fig. 4, H77c/N5BX-JFH1, H77c/N3H+N5BX-JFH1, Con1/N5BX-JFH1, and Con1/N3H+N5BX-JFH1). HCV polyprotein processing is critically important for HCV RNA replication and virus production, and this processing may be affected by the chimeric RNA molecules between different isolates of genotype 2 as well as those between genotypes 1 and 2. However, our data indicated that HCV polyprotein processing did not differ among the chimeric constructs (data not shown). Thus, the JFH-1 N3H and N5BX regions can rescue the replication of genotype 2a replicons at different levels but not the replication of genotype 1 replicons.

The NS3 helicase and NS5B-3′X regions are both important for JFH-1 genomic RNA replication. Next, we applied the previously described results to genomic RNA replication. The structures of HCV, the template DNA for JFH-1, and the chimeric full-genomic RNAs are shown in Fig. 5A. Full-length HCV RNAs were synthesized as described above and their quality and integrity then confirmed by gel electrophoresis (data not shown). To analyze the transient RNA replication of these chimeric RNAs in Huh7 cells, the synthesized RNAs were transfected into Huh7 cells and total RNA was extracted from HCV RNA-transfected cells at various time points. Northern blot analysis was then performed. The equality of the transfection efficiencies was confirmed by the cotransfection of luciferase mRNA (data not shown). As shown in Fig. 5B, JFH-1 RNA decreased at 10 h after transfection but replicated efficiently at 24 to 48 h after transfection, as described previously (48). J6 chimeric RNA with the NS3 helicase and N5BX regions of JFH-1 (J6/N3H+N5BX-JFH1) replicated with similar kinetics but with lower efficiency. J6 chimeric RNA with JFH-1 N5BX (J6/N5BX-JFH1) showed no replication in this assay, like J6CF or JFH-1 GND, although this chimera replicated to a considerable extent in subgenomic-replicon assays. Taken together, these data indicate that the NS3 helicase-coding region and the NS5B-to-3′X region of JFH-1 are both essential for full-length genomic HCV RNA replication in Huh7 cells.

Core protein and infectious-chimeric-virus secretion from chimeric J6CF RNA-transfected cells. Finally, we tested whether chimeric RNA-transfected cells could secrete infectious virus particles. Figure 5C shows the core protein secretion into the culture medium from JFH-1, JFH-1/GND, J6CF, and chimeric-RNA-transfected cells. Core protein was efficiently secreted from cells transfected with JFH-1 RNA (Fig. 5C and Table 1) and those transfected with J6/N3H+N5BX-JFH1 RNA, but with efficiencies lower than that for JFH-1 (Fig. 5C and Table 1). J6/N5BX-JFH1, JFH-1/GND, and J6CF RNA-transfected cells, which showed no RNA replication by Northern blot analysis (Fig. 5B), did not secrete core proteins into the culture medium (Table 1). By the replicon assay, JFH-1/N5BX-J6 showed no replication in Huh7 cells (Fig. 2B, N5BX-J6), and full-length JFH-1/N5BX-J6 RNA-transfected cells did not secrete core protein into the culture medium (Table 1). On the other hand, JFH-1/N5B-J6 replicated to some extent in the replicon assay (Fig. 2B, N5B-J6), and full-length JFH-1/N5B-J6 RNA-transfected cells secreted a smaller amount of core protein than JFH-1 RNA-transfected cells (Fig. 5C and Table 1). Both JFH-1/N3H-J6 and JFH-1/3′UTR-J6 RNA-transfected cells secreted about half the amount of core protein that the JFH-1 RNA-transfected cells did (Fig. 5C and Table 1); however, the replication level of the JFH1/N3H-J6 replicon was markedly lower than those of the JFH-1 and JFH-1/3′UTR-J6 replicons (Fig. 2B, JFH-1 wt, N3H-J6, and 3′UTR-J6), and the replication level of full-length JFH-1/N3H-J6 RNA was also lower than those of the JFH-1 and JFH-1/3′UTR-J6 RNAs as determined by Northern blot analysis (data not shown). Transfection of the other two chimeric RNAs, JFH-1/N3H+N5B-J6 and JFH-1/N3H+N5BX-J6, did not induce core protein secretion (Table 1), and this is in agreement with the finding that neither chimeric replicon replicated (Fig. 2B, N3H+N5B-J6 and N3H+N5BX-J6).

Then, we tested the infectivity of the culture medium from the RNA-transfected cells by a focus formation assay. The infectivity of the culture medium from JFH-1 RNA-transfected cells was determined as $8.8 \times 10^3 \pm 5.7 \times 10^2$ FFU/ml (Table 1). The infectivity of the culture medium was also detected from cells transfected with J6/N3H+N5BX/JFH-1, JFH1/N3H-J6, JFH-1/N5B-J6, or JFH-1/3′UTR-J6 RNA but not with other chimeric RNAs (Table 1). This result thus indicates that efficient core protein secretion is at least indispensable for infectious-virus secretion. However, the levels of infectivity of culture medium did not correlate with core protein concentrations. In particular, JFH-1/N3H-J6 RNA-transfected cells secreted a rather higher level of core protein, but its infectious titer was low. The RNA replication capacity of JFH-1/N3H-J6 was lower than that of wild-type JFH-1 or JFH-1/3′UTR-J6

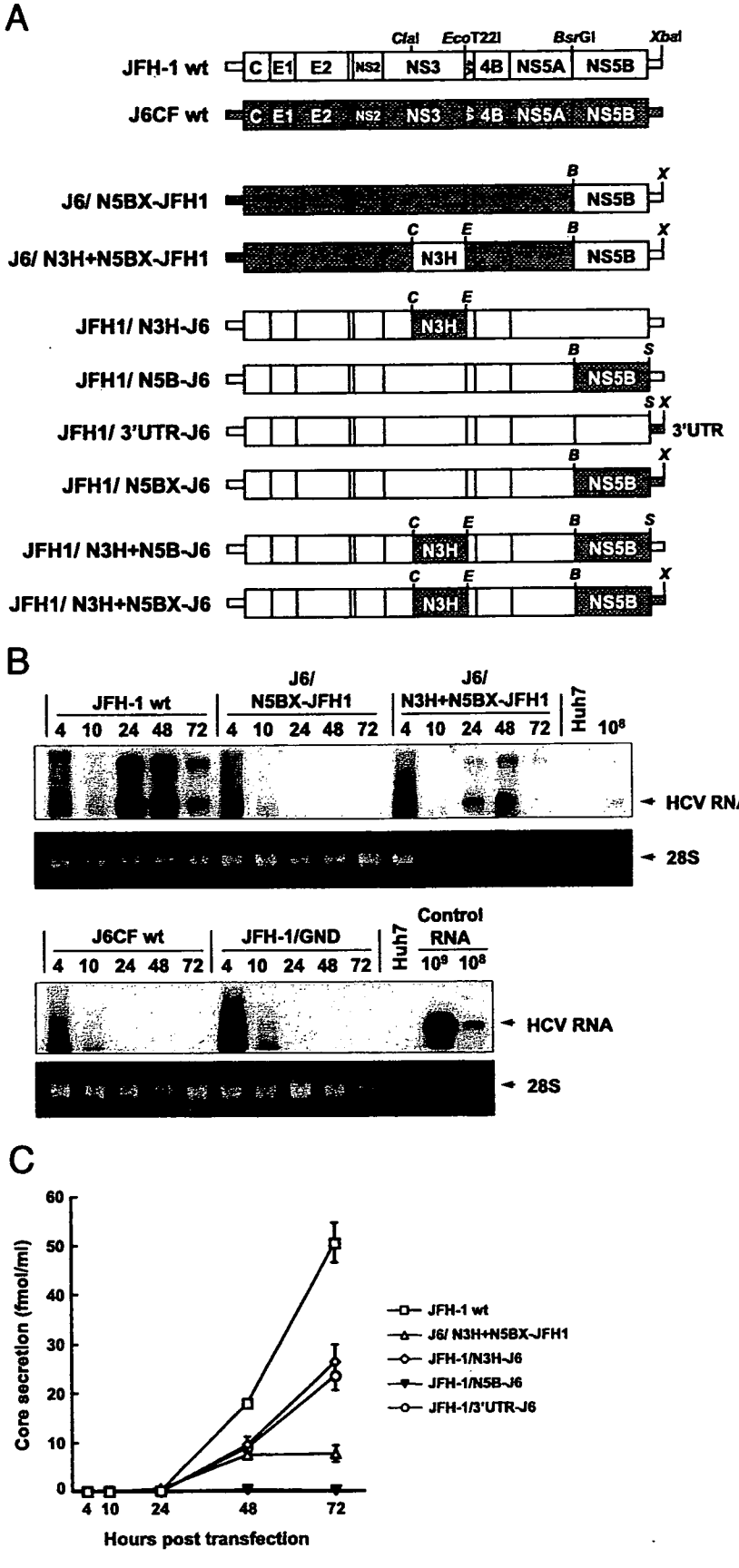
A
ClaI
EcoT22I
BsrGI
XbaI
JFH-1 wt
C E1 E2 NS2 NS3 4B NS5A NS5B
J6CF wt
C E1 E2 NS2 NS3 4B NS5A NS5B
J6/ N5BX-JFH1
J6/ N3H+N5BX-JFH1
JFH1/ N3H-J6
JFH1/ N5B-J6
JFH1/ 3'UTR-J6
3'UTR
JFH1/ N5BX-J6
JFH1/ N3H+N5B-J6
JFH1/ N3H+N5BX-J6
B
JFH-1 wt
J6/ N5BX-JFH1
J6/ N3H+N5BX-JFH1
Huh7
4 10 24 48 72 4 10 24 48 72 4 10 24 48 72
10^8
HCV RNA
28S
J6CF wt
JFH-1/GND
Control RNA
10^9 10^8
C
Core secretion (fmol/ml)
Hours post transfection
JFH-1 wt
J6/ N3H+N5BX-JFH1
JFH-1/N3H-J6
JFH-1/N5B-J6
JFH-1/3'UTR-J6

TABLE 1. Infectious titers of the media from chimeric HCV RNA-transfected cells

Construct[a]	Core protein level (fmol/ml)	Infectivity (FFU/ml)
JFH-1 (wild type)	50.7 ± 4.1	$8.8 \times 10^3 \pm 5.7 \times 10^2$
JFH-1/GND	0	0
J6CF (wild type)	0	0
J6/N5BX-JFH1	0	0
J6/N3H+N5BX-JFH1	7.7 ± 1.7	$9.1 \times 10^1 \pm 4.1 \times 10^1$
JFH-1/N3H-J6	26.3 ± 3.6	$1.7 \times 10^1 \pm 1.2 \times 10^1$
JFH-1/N5B-J6	0.1 ± 0.0	$6.7 \times 10^0 \pm 4.1 \times 10^0$
JFH-1/3'UTR-J6	23.6 ± 2.9	$2.6 \times 10^3 \pm 7.1 \times 10^2$
JFH-1/N5BX-J6	0	0
JFH-1/N3H+N5B-J6	0	0
JFH-1/N3H+N5BX-J6	0	0

[a] Culture media were collected from the RNA-transfected cells 72 h after transfection.

(Fig. 2B), and currently, there is no clear explanation for this discrepancy. This will be further examined in a future study.

Importantly, we found that the J6/N3H+N5BX-JFH1 chimera produced infectious virus. These results strongly indicate that the NS3 helicase and NS5B-to-3'X regions of JFH-1 are important for autonomous replication of the replication-incompetent J6CF strain and for secretion of infectious chimeric virus, although the virus secretion efficiency and the infection efficiency of the secreted virus were low.

DISCUSSION

In the present study, we identified the regions that are important for efficient JFH-1 replication in Huh7 cells by using chimeric constructs with other genotype 2a clones. Via transient replication assays of JFH-1 and J6CF chimeras, both the NS3 helicase-coding (N3H) region and the NS5B-to-3'X (N5BX) region of JFH-1 were found to be important for replication (Fig. 2 and 3). This was also confirmed by full-length genomic RNA replication, but the replication level of J6/N3H+N5BX-JFH1 was lower than that of wild-type JFH-1 (Fig. 5B). The N5BX region of JFH-1 was the minimum essential region for subgenomic-replicon replication (Fig. 3B, N5BX-JFH-1), but in full-length RNA replication, the NS3 helicase-coding region of JFH-1 was also necessary (Fig. 5B). This contradiction might be explained by differences in RNA length, because shorter RNAs such as subgenomic replicons are likely to replicate even with a less powerful replication engine. Alternatively, there could be some negative element for replication in the J6CF structural-protein-coding region or some positive element in the *neo* encephalomyocarditis virus internal ribosome entry site region of the subgenomic replicon. Furthermore, J6 chimeric RNA with the minimum essential regions of JFH-1 (J6/N3H+N5BX-JFH1) caused Huh7 cells to secrete infectious chimeric virus particles. However, the infection efficiency of J6/N3H+N5BX-JFH1 was lower than that of wild-type JFH-1. First, this may be due to the low RNA replication level. With JFH-1 NS3 helicase and N5BX, J6CF was able to replicate, but the replication efficiency was lower than that of JFH-1 (Fig. 5B). Because J6CF replication could occur only with JFH-1 NS3 helicase and N5BX, more *cis*-acting replication elements (CREs) of JFH-1 may be needed for more efficient replication of J6CF. Second, the levels of virus assembly may be low. This chimera had only the NS3 helicase, NS5B, and 3'UTR regions of JFH-1, possibly omitting some regions important for efficient virus particle secretion. Given that the NS2 region of JFH-1 is reportedly important in virus assembly and release (39), the NS2 region may be a possible candidate. JFH-1/N3H-J6 RNA-transfected cells secreted a substantial amount of core protein; however, its infectivity was much lower (Table 1). The JFH-1 N3H region may be important for the infectivity of the secreted virus and/or for virus particle secretion itself. This will be determined in a future study.

Significance of JFH-1 N5BX for replication. We demonstrated the importance of both the NS5B-coding region and the 3'UTR in JFH-1 replication in the present study. There are several reports regarding CREs within the NS5B-coding region and 3'UTR of Con1 (9, 28, 52). The importance of the interaction between CREs in NS5B and the 3'UTR for replication has also been reported for the Con1 strain (9). The nucleotide sequences involved in the kissing-loop interaction were conserved between JFH-1, J6CF, and Con-1. However, mutations in other regions may affect this interaction by disrupting the RNA secondary structures. On the other hand, given that the NS5B-coding region encodes an RNA-dependent RNA polymerase, the enzymatic activities of the polymerase may differ among the tested strains. The sequence similarities of the JFH-1 and J6CF NS5B regions are 92.2% for the nucleotide sequence and 95.1% for the amino acid sequence. Out of 591 amino acids, only 29 amino acids differ, and the GDD motif that is highly conserved among RdRps is conserved. There are many reports regarding the interaction between NS5B and other viral or cellular proteins, and some of the interactions have been reported to play a role in replication (6, 10, 12, 15, 17, 27, 41–43, 45, 46). Furthermore, the importance of the membrane localization of NS5B with respect to replication has also been reported (29, 35). Mutations in J6CF NS5B may affect these roles. It is thus important to examine the RdRp activities of JFH-1 and J6CF NS5B proteins in vitro.

FIG. 5. Analysis of transient replication of genomic chimeric HCV RNA. (A) Structures of full-length chimeric HCV RNAs. Each chimeric full-length construct was prepared by the insertion of the restricted fragments as indicated. The restriction enzyme recognition sites used for the plasmid constructions are indicated. *C*, ClaI; *E*, EcoT22I; *B*, BsrGI; *S*, StuI; *X*, XbaI; wt, wild type. (B) Northern blot analysis of total RNA prepared from cells transfected with transcribed genomic HCV RNA. Numbers of synthetic JFH-1 RNA (control RNA), RNA isolated from naïve cells (Huh7), and hours after transfection (4, 10, 24, 48, and 72) are indicated. Arrowheads indicate full-length HCV RNA (HCV RNA) and 28S rRNA (28S). A representative autoradiogram (6-h exposure) of three independent experiments is presented. (C) HCV core protein secretion from the RNA-transfected cells. Transcribed wild-type or chimeric full-length HCV RNAs (10 μg) were transfected into Huh7 cells. Culture medium was harvested at 4, 10, 24, 48, and 72 h after transfection. The amounts of core proteins in the harvested culture medium were measured using an HCV core enzyme-linked immunosorbent assay. The assays were performed five times independently, and data are presented as means and standard deviations.

On the other hand, the effect of the 3'UTR is very surprising, especially since the nucleotide sequences of this region are very similar between JFH-1 and J6CF. In this study, the 3'UTR includes four parts: 22 nucleotides at the 3'-end NS5B region (as a result of the cloning strategy), 39 nucleotides of variable region, the poly(U/UC) region, and a 98-nucleotide 3'X region. There are a single synonymous nucleotide mutation in the 3'-end NS5B region and three nucleotide mutations in the variable region. The poly(U/UC) regions are 99 and 132 nucleotides in JFH-1 and J6CF, respectively. There are no mutations in the 3'X region in either strain. It is thus quite interesting to pursue the mechanisms of these mutations in the 3'UTR that affect the HCV RNA replication levels. Further studies are important for precise elucidation of the efficient replication mechanisms of JFH-1.

Significance of the JFH-1 NS3 helicase region for replication. In the present study, we demonstrated the importance of the JFH-1 NS3 helicase region, especially in full-length genomic RNA replication. It has been reported that an active NS3 helicase is required for replication of subgenomic replicons (25). The NS3 helicase domain possesses helicase activity and ATPase activity, and it has been reported that the characters of these enzymes differ among the genotypes and the strains (26). NS3 has also been reported to interact with positive- and negative-strand RNA 3'UTRs (1). One possible model of the role of NS3 in RNA replication is that NS3 helicase unwinds RNA secondary structures and/or a double-stranded RNA intermediate before RNA synthesis by NS5B (37). The sequence similarity of the NS3 helicase regions of JFH-1 and J6CF is rather high, 89.5% for the nucleotide sequence and 93.8% for the amino acid sequence, and out of 487 amino acids, only 30 amino acids differ. These mutations may affect the enzymatic activities of NS3 helicase.

Furthermore, it has been reported that NS3 can stimulate NS5B RdRp activity (38). It has also been reported that the NS3 protease domain and NS5B stimulate NS3 helicase activity (53). Taken together, these findings show that not only the enzymatic activities themselves but also the combination or interaction of the NS3 and NS5B proteins could be important. However, it is still important to examine and compare the NS3 helicase enzymatic activities in vitro of JFH-1 and other HCV strains in a further study.

Replication in vitro and in vivo. We previously reported that JFH-1 RNA could replicate efficiently in Huh7 cells. Cell-cultured JFH-1 virus was also found to be infectious in chimpanzees; however, the virus was cleared immediately after transient viremia (48). In contrast, J6CF does not replicate in Huh7 cells, but it is infectious in chimpanzees (49). J6/JFH-1 chimeric RNA replicated efficiently in Huh7 cells (39) and Huh7-derived cell lines (30), and cell-cultured chimeric J6/JFH-1 virus was infectious in chimpanzees and in chimeric uPA-SCID mice (31). Replication efficiency in vitro may not necessarily correlate with that in vivo. The H77, Con-1, and HCV-N strains were infectious in chimpanzees (3, 5, 23, 50). However, the H77 and Con-1 strains need adaptive mutations for efficient replication in cultured cells (4, 24) and HCV-N replicates relatively efficiently in cultured cells (16). On the other hand, H77-S containing five adaptive mutations can produce infectious virus particles (51), but the Con-1 and HCV-N strains do not produce virus particles (16, 40). It is still unclear what viral or host factors are important for efficient replication and infectious-virus production in vitro and in vivo. However, understanding HCV replication mechanisms by using cell culture models is still important for elucidation of the HCV life cycle.

Significance of the regions responsible for JFH-1 replication. Using two HCV strains, JFH-1 and J6CF, which are very closely related but have different characteristics, we were able to determine which regions are important for replication in cultured cells. Replication of two other genotype 2a strains, JCH-1 and JCH-4, was also recovered by replacement of the N3H and N5BX regions of JFH-1 at the lower levels compared to replication of the J6 replicon (Fig. 3B and 4). This may be because J6CF is an infectious clone in chimpanzees, but the JCH-1 and JCH-4 strains are clinical isolates from chronic-hepatitis patients (21) and may include critical mutations in other important regions. Furthermore, replication of genotype 1 HCV replicons was not restored by the same procedure as that for genotype 2a replicons (Fig. 4). Functional complementation in the nonstructural region and 3'UTR may be difficult beyond the genotypes.

Obtaining virus particles is an important step in antiviral research. Although infection efficiency is improved in permissive cell lines, most HCV strains still cannot replicate or produce virus particles in cultured cells. Therefore, chimeric virus particles with the JFH-1 replication engine may be suitable substitutes. Furthermore, analyses using chimeric viruses that have structural proteins and other regions from various strains may give us new information regarding strain-specific effects on HCV life cycles. Consequently, applying the findings of the present study to replication-incompetent strains may be useful not only for analyses of virus strain specificity and precise analyses of the HCV life cycle but also for antiviral studies.

In conclusion, we analyzed the mechanism underlying efficient JFH-1 replication by using intragenotypic chimeras of JFH-1 and J6CF and clearly showed the importance of the JFH-1 NS3 helicase region and the NS5B-to-3'X region for efficient replication of HCV genotype 2a strains.

ACKNOWLEDGMENTS

A.M. is supported by the Viral Hepatitis Research Foundation of Japan, and K.M. is supported by the Japan Health Sciences Foundation. This work was partially supported by a grant-in-aid for Scientific Research from the Japan Society for the Promotion of Science, from the Ministry of Health, Labor and Welfare of Japan, and from the Ministry of Education, Culture, Sports, Science and Technology and by the Research on Health Sciences Focusing on Drug Innovation from the Japan Health Sciences Foundation.

The pJ6CF plasmid was kindly provided by Jens Bukh. The pCV-H77c plasmid was kindly provided by Robert H. Purcell. The pFK-I389/neo/NS3-3'/wt plasmid was kindly provided by Ralf Bartenschlager.

REFERENCES

1. Banerjee, R., and A. Dasgupta. 2001. Specific interaction of hepatitis C virus protease/helicase NS3 with the 3'-terminal sequences of viral positive- and negative-strand RNA. J. Virol. 75:1708–1721.
2. Bartenschlager, R., and V. Lohmann. 2000. Replication of hepatitis C virus. J. Gen. Virol. 81:1631–1648.
3. Beard, M. R., G. Abell, M. Honda, A. Carroll, M. Gartland, B. Clarke, K. Suzuki, R. Lanford, D. V. Sangar, and S. M. Lemon. 1999. An infectious molecular clone of a Japanese genotype 1b hepatitis C virus. Hepatology 30:316–324.
4. Blight, K. J., J. A. McKeating, J. Marcotrigiano, and C. M. Rice. 2003.

Efficient replication of hepatitis C virus genotype 1a RNAs in cell culture. J. Virol. 77:3181–3190.
5. **Bukh, J., T. Pietschmann, V. Lohmann, N. Krieger, K. Faulk, R. E. Engle, S. Govindarajan, M. Shapiro, M. St. Claire, and R. Bartenschlager.** 2002. Mutations that permit efficient replication of hepatitis C virus RNA in Huh-7 cells prevent productive replication in chimpanzees. Proc. Natl. Acad. Sci. USA 99:14416–14421.
6. **Choi, S. H., K. J. Park, B. Y. Ahn, G. Jung, M. M. Lai, and S. B. Hwang.** 2006. Hepatitis C virus nonstructural 5B protein regulates tumor necrosis factor alpha signaling through effects on cellular IκB kinase. Mol. Cell. Biol. 26:3048–3059.
7. **Choo, Q. L., G. Kuo, A. J. Weiner, L. R. Overby, D. W. Bradley, and M. Houghton.** 1989. Isolation of a cDNA clone derived from a blood-borne non-A, non-B viral hepatitis genome. Science 244:359–362.
8. **Choo, Q. L., K. H. Richman, J. H. Han, K. Berger, C. Lee, C. Dong, C. Gallegos, D. Coit, R. Medina-Selby, P. J. Barr, et al.** 1991. Genetic organization and diversity of the hepatitis C virus. Proc. Natl. Acad. Sci. USA 88:2451–2455.
9. **Friebe, P., J. Boudet, J. P. Simorre, and R. Bartenschlager.** 2005. Kissing-loop interaction in the 3′ end of the hepatitis C virus genome essential for RNA replication. J. Virol. 79:380–392.
10. **Gao, L., H. Tu, S. T. Shi, K. J. Lee, M. Asanaka, S. B. Hwang, and M. M. Lai.** 2003. Interaction with a ubiquitin-like protein enhances the ubiquitination and degradation of hepatitis C virus RNA-dependent RNA polymerase. J. Virol. 77:4149–4159.
11. **Grakoui, A., C. Wychowski, C. Lin, S. M. Feinstone, and C. M. Rice.** 1993. Expression and identification of hepatitis C virus polyprotein cleavage products. J. Virol. 67:1385–1395.
12. **Hamamoto, I., Y. Nishimura, T. Okamoto, H. Aizaki, M. Liu, Y. Mori, T. Abe, T. Suzuki, M. M. Lai, T. Miyamura, K. Moriishi, and Y. Matsuura.** 2005. Human VAP-B is involved in hepatitis C virus replication through interaction with NS5A and NS5B. J. Virol. 79:13473–13482.
13. **Hijikata, M., N. Kato, Y. Ootsuyama, M. Nakagawa, and K. Shimotohno.** 1991. Gene mapping of the putative structural region of the hepatitis C virus genome by in vitro processing analysis. Proc. Natl. Acad. Sci. USA 88:5547–5551.
14. **Hijikata, M., H. Mizushima, Y. Tanji, Y. Komoda, Y. Hirowatari, T. Akagi, N. Kato, K. Kimura, and K. Shimotohno.** 1993. Proteolytic processing and membrane association of putative nonstructural proteins of hepatitis C virus. Proc. Natl. Acad. Sci. USA 90:10773–10777.
15. **Hirano, M., S. Kaneko, T. Yamashita, H. Luo, W. Qin, Y. Shirota, T. Nomura, K. Kobayashi, and S. Murakami.** 2003. Direct interaction between nucleolin and hepatitis C virus NS5B. J. Biol. Chem. 278:5109–5115.
16. **Ikeda, M., M. Yi, K. Li, and S. M. Lemon.** 2002. Selectable subgenomic and genome-length dicistronic RNAs derived from an infectious molecular clone of the HCV-N strain of hepatitis C virus replicate efficiently in cultured Huh7 cells. J. Virol. 76:2997–3006.
17. **Ishido, S., T. Fujita, and H. Hotta.** 1998. Complex formation of NS5B with NS3 and NS4A proteins of hepatitis C virus. Biochem. Biophys. Res. Commun. 244:35–40.
18. **Kato, N., M. Hijikata, Y. Ootsuyama, M. Nakagawa, S. Ohkoshi, T. Sugimura, and K. Shimotohno.** 1990. Molecular cloning of the human hepatitis C virus genome from Japanese patients with non-A, non-B hepatitis. Proc. Natl. Acad. Sci. USA 87:9524–9528.
19. **Kato, T., T. Date, M. Miyamoto, A. Furusaka, K. Tokushige, M. Mizokami, and T. Wakita.** 2003. Efficient replication of the genotype 2a hepatitis C virus subgenomic replicon. Gastroenterology 125:1808–1817.
20. **Kato, T., T. Date, M. Miyamoto, M. Sugiyama, Y. Tanaka, E. Orito, T. Ohno, K. Sugihara, I. Hasegawa, K. Fujiwara, K. Ito, A. Ozasa, M. Mizokami, and T. Wakita.** 2005. Detection of anti-hepatitis C virus effects of interferon and ribavirin by a sensitive replicon system. J. Clin. Microbiol. 43:5679–5684.
21. **Kato, T., A. Furusaka, M. Miyamoto, T. Date, K. Yasui, J. Hiramoto, K. Nagayama, T. Tanaka, and T. Wakita.** 2001. Sequence analysis of hepatitis C virus isolated from a fulminant hepatitis patient. J. Med. Virol. 64:334–339.
22. **Kiyosawa, K., T. Sodeyama, E. Tanaka, Y. Gibo, K. Yoshizawa, Y. Nakano, S. Furuta, Y. Akahane, K. Nishioka, R. H. Purcell, et al.** 1990. Interrelationship of blood transfusion, non-A, non-B hepatitis and hepatocellular carcinoma: analysis by detection of antibody to hepatitis C virus. Hepatology 12:671–675.
23. **Kolykhalov, A. A., E. V. Agapov, K. J. Blight, K. Mihalik, S. M. Feinstone, and C. M. Rice.** 1997. Transmission of hepatitis C by intrahepatic inoculation with transcribed RNA. Science 277:570–574.
24. **Krieger, N., V. Lohmann, and R. Bartenschlager.** 2001. Enhancement of hepatitis C virus RNA replication by cell culture-adaptive mutations. J. Virol. 75:4614–4624.
25. **Lam, A. M., and D. N. Frick.** 2006. Hepatitis C virus subgenomic replicon requires an active NS3 RNA helicase. J. Virol. 80:404–411.
26. **Lam, A. M., D. Keeney, P. Q. Eckert, and D. N. Frick.** 2003. Hepatitis C virus NS3 ATPases/helicases from different genotypes exhibit variations in enzymatic properties. J. Virol. 77:3950–3961.
27. **Lan, S., H. Wang, H. Jiang, H. Mao, X. Liu, X. Zhang, Y. Hu, L. Xiang, and Z. Yuan.** 2003. Direct interaction between alpha-actinin and hepatitis C virus NS5B. FEBS Lett. 554:289–294.
28. **Lee, H., H. Shin, E. Wimmer, and A. V. Paul.** 2004. *cis*-Acting RNA signals in the NS5B C-terminal coding sequence of the hepatitis C virus genome. J. Virol. 78:10865–10877.
29. **Lee, K. J., J. Choi, J. H. Ou, and M. M. Lai.** 2004. The C-terminal transmembrane domain of hepatitis C virus (HCV) RNA polymerase is essential for HCV replication in vivo. J. Virol. 78:3797–3802.
30. **Lindenbach, B. D., M. J. Evans, A. J. Syder, B. Wolk, T. L. Tellinghuisen, C. C. Liu, T. Maruyama, R. O. Hynes, D. R. Burton, J. A. McKeating, and C. M. Rice.** 2005. Complete replication of hepatitis C virus in cell culture. Science 309:623–626.
31. **Lindenbach, B. D., P. Meuleman, A. Ploss, T. Vanwolleghem, A. J. Syder, J. A. McKeating, R. E. Lanford, S. M. Feinstone, M. E. Major, G. Leroux-Roels, and C. M. Rice.** 2006. Cell culture-grown hepatitis C virus is infectious in vivo and can be recultured in vitro. Proc. Natl. Acad. Sci. USA 103:3805–3809.
32. **Lohmann, V., F. Korner, J. Koch, U. Herian, L. Theilmann, and R. Bartenschlager.** 1999. Replication of subgenomic hepatitis C virus RNAs in a hepatoma cell line. Science 285:110–113.
33. **McLauchlan, J., M. K. Lemberg, G. Hope, and B. Martoglio.** 2002. Intramembrane proteolysis promotes trafficking of hepatitis C virus core protein to lipid droplets. EMBO J. 21:3980–3988.
34. **Miyamoto, M., T. Kato, T. Date, M. Mizokami, and T. Wakita.** 2006. Comparison between subgenomic replicons of hepatitis C virus genotypes 2a (JFH-1) and 1b (Con1 NK5.1). Intervirology 49:37–43.
35. **Moradpour, D., V. Brass, E. Bieck, P. Friebe, R. Gosert, H. E. Blum, R. Bartenschlager, F. Penin, and V. Lohmann.** 2004. Membrane association of the RNA-dependent RNA polymerase is essential for hepatitis C virus RNA replication. J. Virol. 78:13278–13284.
36. **Nakabayashi, H., K. Taketa, K. Miyano, T. Yamane, and J. Sato.** 1982. Growth of human hepatoma cells lines with differentiated functions in chemically defined medium. Cancer Res. 42:3858–3863.
37. **Paolini, C., R. De Francesco, and P. Gallinari.** 2000. Enzymatic properties of hepatitis C virus NS3-associated helicase. J. Gen. Virol. 81:1335–1345.
38. **Piccininni, S., A. Varaklioti, M. Nardelli, B. Dave, K. D. Raney, and J. E. McCarthy.** 2002. Modulation of the hepatitis C virus RNA-dependent RNA polymerase activity by the non-structural (NS) 3 helicase and the NS4B membrane protein. J. Biol. Chem. 277:45670–45679.
39. **Pietschmann, T., A. Kaul, G. Koutsoudakis, A. Shavinskaya, S. Kallis, E. Steinmann, K. Abid, F. Negro, M. Dreux, F. L. Cosset, and R. Bartenschlager.** 2006. Construction and characterization of infectious intragenotypic and intergenotypic hepatitis C virus chimeras. Proc. Natl. Acad. Sci. USA 103:7408–7413.
40. **Pietschmann, T., V. Lohmann, A. Kaul, N. Krieger, G. Rinck, G. Rutter, D. Strand, and R. Bartenschlager.** 2002. Persistent and transient replication of full-length hepatitis C virus genomes in cell culture. J. Virol. 76:4008–4021.
41. **Shimakami, T., M. Hijikata, H. Luo, Y. Y. Ma, S. Kaneko, K. Shimotohno, and S. Murakami.** 2004. Effect of interaction between hepatitis C virus NS5A and NS5B on hepatitis C virus RNA replication with the hepatitis C virus replicon. J. Virol. 78:2738–2748.
42. **Shimakami, T., M. Honda, T. Kusakawa, T. Murata, K. Shimotohno, S. Kaneko, and S. Murakami.** 2006. Effect of hepatitis C virus (HCV) NS5B-nucleolin interaction on HCV replication with HCV subgenomic replicon. J. Virol. 80:3332–3340.
43. **Shirota, Y., H. Luo, W. Qin, S. Kaneko, T. Yamashita, K. Kobayashi, and S. Murakami.** 2002. Hepatitis C virus (HCV) NS5A binds RNA-dependent RNA polymerase (RdRP) NS5B and modulates RNA-dependent RNA polymerase activity. J. Biol. Chem. 277:11149–11155.
44. **Takamizawa, A., C. Mori, I. Fuke, S. Manabe, S. Murakami, J. Fujita, E. Onishi, T. Andoh, I. Yoshida, and H. Okayama.** 1991. Structure and organization of the hepatitis C virus genome isolated from human carriers. J. Virol. 65:1105–1113.
45. **Tu, H., L. Gao, S. T. Shi, D. R. Taylor, T. Yang, A. K. Mircheff, Y. Wen, A. E. Gorbalenya, S. B. Hwang, and M. M. Lai.** 1999. Hepatitis C virus RNA polymerase and NS5A complex with a SNARE-like protein. Virology 263:30–41.
46. **Uchida, M., N. Hino, T. Yamanaka, H. Fukushima, T. Imanishi, Y. Uchiyama, T. Kodama, and T. Doi.** 2002. Hepatitis C virus core protein binds to a C-terminal region of NS5B RNA polymerase. Hepatol. Res. 22:297–306.
47. **van den Hoff, M. J., A. F. Moorman, and W. H. Lamers.** 1992. Electroporation in 'intracellular' buffer increases cell survival. Nucleic Acids Res. 20:2902.
48. **Wakita, T., T. Pietschmann, T. Kato, T. Date, M. Miyamoto, Z. Zhao, K. Murthy, A. Habermann, H. G. Krausslich, M. Mizokami, R. Bartenschlager, and T. J. Liang.** 2005. Production of infectious hepatitis C virus in tissue culture from a cloned viral genome. Nat. Med. 11:791–796.
49. **Yanagi, M., R. H. Purcell, S. U. Emerson, and J. Bukh.** 1999. Hepatitis C virus: an infectious molecular clone of a second major genotype (2a) and lack of viability of intertypic 1a and 2a chimeras. Virology 262:250–263.
50. **Yanagi, M., R. H. Purcell, S. U. Emerson, and J. Bukh.** 1997. Transcripts

from a single full-length cDNA clone of hepatitis C virus are infectious when directly transfected into the liver of a chimpanzee. Proc. Natl. Acad. Sci. USA 94:8738–8743.
51. Yi, M., R. A. Villanueva, D. L. Thomas, T. Wakita, and S. M. Lemon. 2006. Production of infectious genotype 1a hepatitis C virus (Hutchinson strain) in cultured human hepatoma cells. Proc. Natl. Acad. Sci. USA 103:2310–2315.
52. You, S., D. D. Stump, A. D. Branch, and C. M. Rice. 2004. A *cis*-acting replication element in the sequence encoding the NS5B RNA-dependent RNA polymerase is required for hepatitis C virus RNA replication. J. Virol. 78:1352–1366.
53. Zhang, C., Z. Cai, Y. C. Kim, R. Kumar, F. Yuan, P. Y. Shi, C. Kao, and G. Luo. 2005. Stimulation of hepatitis C virus (HCV) nonstructural protein 3 (NS3) helicase activity by the NS3 protease domain and by HCV RNA-dependent RNA polymerase. J. Virol. 79:8687–8697.
54. Zhong, J., P. Gastaminza, G. Cheng, S. Kapadia, T. Kato, D. R. Burton, S. F. Wieland, S. L. Uprichard, T. Wakita, and F. V. Chisari. 2005. Robust hepatitis C virus infection in vitro. Proc. Natl. Acad. Sci. USA 102:9294–9299.

Critical role of PA28γ in hepatitis C virus-associated steatogenesis and hepatocarcinogenesis

Kohji Moriishi*, Rika Mochizuki*, Kyoji Moriya†, Hironobu Miyamoto*, Yoshio Mori*, Takayuki Abe*, Shigeo Murata‡, Keiji Tanaka‡, Tatsuo Miyamura§, Tetsuro Suzuki§, Kazuhiko Koike†, and Yoshiharu Matsuura*¶

*Department of Molecular Virology, Research Institute for Microbial Diseases, Osaka University, Osaka 565-0871, Japan; †Department of Internal Medicine, Graduate School of Medicine, University of Tokyo, Tokyo 113-8655, Japan; ‡Department of Molecular Oncology, Tokyo Metropolitan Institute of Medical Science, Tokyo 113-8613, Japan; and §Department of Virology II, National Institute of Infectious Diseases, Tokyo 162-8640, Japan

Edited by Peter Palese, Mount Sinai School of Medicine, New York, NY, and approved December 1, 2006 (received for review August 23, 2006)

Hepatitis C virus (HCV) is a major cause of chronic liver disease that frequently leads to steatosis, cirrhosis, and eventually hepatocellular carcinoma (HCC). HCV core protein is not only a component of viral particles but also a multifunctional protein because liver steatosis and HCC are developed in HCV core gene-transgenic (CoreTg) mice. Proteasome activator PA28γ/REGγ regulates host and viral proteins such as nuclear hormone receptors and HCV core protein. Here we show that a knockout of the PA28γ gene induces the accumulation of HCV core protein in the nucleus of hepatocytes of CoreTg mice and disrupts development of both hepatic steatosis and HCC. Furthermore, the genes related to fatty acid biosynthesis and *srebp-1c* promoter activity were up-regulated by HCV core protein in the cell line and the mouse liver in a PA28γ-dependent manner. Heterodimer composed of liver X receptor α (LXRα) and retinoid X receptor α (RXRα) is known to up-regulate *srebp-1c* promoter activity. Our data also show that HCV core protein enhances the binding of LXRα/RXRα to LXR-response element in the presence but not the absence of PA28γ. These findings suggest that PA28γ plays a crucial role in the development of liver pathology induced by HCV infection.

fatty acid | proteasome | sterol regulatory element-binding protein (SREBP) | RXRα | LXRα

Hepatitis C virus (HCV) belongs to the Flaviviridae family, and it possesses a positive, single-stranded RNA genome that encodes a single polyprotein composed of ≈3,000 aa. The HCV polyprotein is processed by host and viral proteases, resulting in 10 viral proteins. Viral structural proteins, including the capsid (core) protein and two envelope proteins, are located in the N-terminal one-third of the polyprotein, followed by nonstructural proteins.

HCV infects >170 million individuals worldwide, and then it causes liver disease, including hepatic steatosis, cirrhosis, and eventually hepatocellular carcinoma (HCC) (1). The prevalence of fatty infiltration in the livers of chronic hepatitis C patients has been reported to average ≈50% (2, 3), which is higher than the percentage in patients infected with hepatitis B virus and other liver diseases. However, the precise functions of HCV proteins in the development of fatty liver remain unknown because of the lack of a system sufficient to investigate the pathogenesis of HCV. HCV core protein expression has been shown to induce lipid droplets in cell lines and hepatic steatosis and HCC in transgenic mice (4–6). These reports suggest that HCV core protein plays an important role in the development of various types of liver failure, including steatosis and HCC.

Recent reports suggest that lipid biosynthesis affects HCV replication (7–9). Involvement of a geranylgeranylated host protein, FBL2, in HCV replication through the interaction with NS5A suggests that the cholesterol biosynthesis pathway is also important for HCV replication (9). Increases in saturated and monounsaturated fatty acids enhance HCV RNA replication, whereas increases in polyunsaturated fatty acids suppress it (7). Lipid homeostasis is regulated by a family of steroid regulatory element-binding proteins (SREBPs), which activate the expression of >30 genes involved in the synthesis and uptake of cholesterol, fatty acids, triglycerides, and phospholipids. Biosynthesis of cholesterol is regulated by SREBP-2, whereas that of fatty acids, triglycerides, and phospholipids is regulated by SREBP-1c (10–14). In chimpanzees, host genes involved in SREBP signaling are induced during the early stages of HCV infection (8). SREBP-1c regulates the transcription of acetyl-CoA carboxylase, fatty acid synthase, and stearoyl-CoA desaturase, leading to the production of saturated and monounsaturated fatty acids and triglycerides (15). SREBP-1c is transcriptionally regulated by liver X receptor (LXR) α and retinoid X receptor (RXR) α, which belong to a family of nuclear hormone receptors (15, 16). Accumulation of cellular fatty acids by HCV core protein is expected to be modulated by the SREBP-1c pathway because RXRα is activated by HCV core protein (17). However, it remains unknown whether HCV core protein regulates the *srebp-1c* promoter.

We previously reported (18) that HCV core protein specifically binds to the proteasome activator PA28γ/REGγ in the nucleus and is degraded through a PA28γ-dependent pathway. PA28γ is well conserved from invertebrates to vertebrates, and amino acid sequences of human and murine PA28γs are identical (19). The homologous proteins, PA28α and PA28β, form a heteroheptamer in the cytoplasm, and they activate chymotrypsin-like peptidase activity of the 20S proteasome, whereas PA28γ forms a homoheptamer in the nucleus, and it enhances trypsin-like peptidase activity of 20S proteasome (20). Recently, Li and colleagues (21) reported that PA28γ binds to steroid receptor coactivator-3 (SRC-3) and enhances the degradation of SRC-3 in a ubiquitin- and ATP-independent manner. However, the precise physiological functions of PA28γ are largely unknown *in vivo*. In this work, we examine whether PA28γ is required for liver pathology induced by HCV core protein *in vivo*.

Results

PA28γ-Knockout HCV Core Gene Transgenic Mice. To determine the role of PA28γ in HCV core-induced steatosis and the development of HCC *in vivo*, we prepared PA28γ-knockout core gene transgenic mice. The PA28γ-deficient, PA28γ$^{-/-}$ mice were born without

Author contributions: K. Moriishi, K.T., T.M., T.S., K.K., and Y. Matsuura designed research; K. Moriishi, R.M., K. Moriya, H.M., Y. Mori, and T.A. performed research; S.M. contributed new reagents/analytic tools; Y. Matsuura analyzed data; and K. Moriishi, K.K., and Y. Matsuura wrote the paper.

The authors declare no conflict of interest.

This article is a PNAS direct submission.

Freely available online through the PNAS open access option.

Abbreviations: CoreTg, HCV core gene-transgenic; HCC, hepatocellular carcinoma; HCV, hepatitis C virus; LXR, liver X receptor; LXRE, liver X receptor-response element; MEF, mouse embryonic fibroblast; ROS, reactive oxygen species; RXR, retinoid X receptor; SRC-3, steroid receptor coactivator-3; SREBP, steroid regulatory element-binding protein.

¶To whom correspondence should be addressed. E-mail: matsuura@biken.osaka-u.ac.jp.

This article contains supporting information online at www.pnas.org/cgi/content/full/0607312104/DC1.

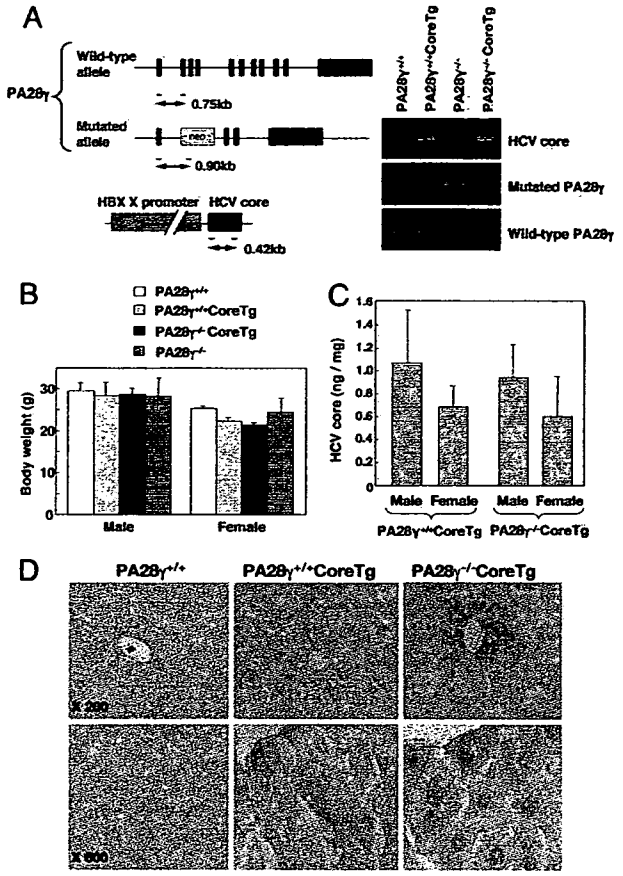

Fig. 1. Preparation and characterization of PA28γ-knockout HCV core-transgenic mice. (*A*) The structures of the wild-type and mutated PA28γ genes and the transgene encoding the HCV core protein under the control of the HBV X promoter were investigated. Positions corresponding to the screening primers and sizes of PCR products are shown. PCR products of the HCV core gene as well as wild-type and mutated PA28γ alleles were amplified from the genomic DNAs of PA28$\gamma^{+/+}$, PA28$\gamma^{+/+}$CoreTg, PA28$\gamma^{-/-}$, and PA28$\gamma^{-/-}$CoreTg mice. (*B*) Body weights of PA28$\gamma^{+/+}$, PA28$\gamma^{+/+}$CoreTg, PA28$\gamma^{-/-}$CoreTg, and PA28$\gamma^{-/-}$ mice at the age of 6 months. (*C*) HCV core protein levels in the livers of PA28$\gamma^{+/+}$CoreTg and PA28$\gamma^{-/-}$CoreTg mice were determined by ELISA (mean ± SD, n = 10). (*D*) Localization of HCV core protein in the liver. Liver sections of PA28$\gamma^{+/+}$, PA28$\gamma^{+/+}$CoreTg, and PA28$\gamma^{-/-}$CoreTg mice at the age of 2 months were stained with anti-HCV core antibody.

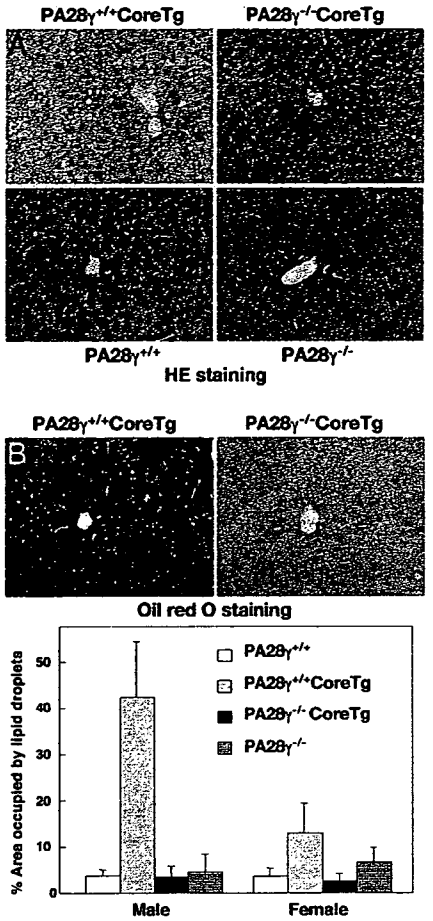

Fig. 2. Accumulation of lipid droplets by expression of HCV core protein. (*A*) Liver sections of the mice at the age of 6 months were stained with hematoxylin/eosin (HE). (*B*) (*Upper*) Liver sections of PA28$\gamma^{+/+}$CoreTg and PA28$\gamma^{-/-}$CoreTg mice at the age of 6 months were stained with oil red O. (*Lower*) The area occupied by lipid droplets of PA28$\gamma^{+/+}$ (white), PA28$\gamma^{+/+}$CoreTg (gray), PA28$\gamma^{-/-}$CoreTg (black), and PA28$\gamma^{-/-}$ (dark gray) mice was calculated by Image-Pro software (MediaCybernetics, Silver Spring, MD) (mean ± SD, n = 10).

appreciable abnormalities in all tissues examined, with the exception of a slight retardation of growth (22). HCV core gene-transgenic (PA28$\gamma^{+/+}$CoreTg) mice were bred with PA28$\gamma^{-/-}$ mice to create PA28$\gamma^{+/-}$CoreTg mice. The PA28$\gamma^{+/-}$CoreTg offspring were bred with each other, and PA28$\gamma^{-/-}$CoreTg mice were selected by PCR using primers specific to the target sequences (Fig. 1*A*). No significant differences in body weight were observed among the 6-month-old mice, although PA28$\gamma^{-/-}$ mice exhibited a slight retardation of growth (Fig. 1*B*). A similar level of PA28γ expression was detected in PA28$\gamma^{+/+}$CoreTg and PA28$\gamma^{+/+}$ mice (see Fig. 5*B*). The expression levels and molecular size of HCV core protein were similar in the livers of PA28$\gamma^{+/+}$CoreTg and PA28$\gamma^{-/-}$CoreTg mice (Fig. 1*C*; see also Fig. 5*B*).

PA28γ Is Required for Degradation of HCV Core Protein in the Nucleus and Induction of Liver Steatosis. HCV core protein has been detected at various sites, such as the endoplasmic reticulum, mitochondria, lipid droplets, and nucleus of cultured cell lines, as well as in hepatocytes of PA28$\gamma^{+/+}$CoreTg mice and hepatitis C patients (6, 23, 24). Although HCV core protein is predominantly detected in the cytoplasm of the liver cells of PA28$\gamma^{+/+}$CoreTg mice, as reported in ref. 6, in the present study a clear accumulation of HCV core protein was observed in the liver cell nuclei of PA28$\gamma^{-/-}$CoreTg mice (Fig. 1*D*). These findings clearly indicate that at least some fraction of the HCV core protein is translocated into the nucleus and is degraded through a PA28γ-dependent pathway. Mild vacuolation was observed in the cytoplasm of the liver cells of 4-month-old PA28$\gamma^{+/+}$CoreTg mice, and it became more severe at 6 months, as reported in ref. 25. Hematoxylin/eosin-stained liver sections of 6-month-old PA28$\gamma^{+/+}$CoreTg mice exhibited severe vacuolating lesions (Fig. 2*A*), which were clearly stained with oil red O (Fig. 2*B Upper*), whereas no such lesions were detected in the livers of PA28$\gamma^{-/-}$CoreTg, PA28$\gamma^{+/+}$, or PA28$\gamma^{-/-}$ mice at the same age. The areas occupied by the lipid droplets in the PA28$\gamma^{+/+}$CoreTg mouse livers were ≈10 and 2–4 times larger than those of male and female of PA28$\gamma^{+/+}$, PA28$\gamma^{-/-}$, and PA28$\gamma^{-/-}$CoreTg mice, respectively (Fig. 2*B Lower*). These results suggest that PA28γ is required for the induction of liver steatosis by HCV core protein in mice.

PA28γ Is Required for the Up-Regulation of SREBP-1c Transcription by HCV Core Protein in the Mouse Liver. To clarify the effects of a knockout of the PA28γ gene in PA28$\gamma^{+/+}$CoreTg mice on lipid

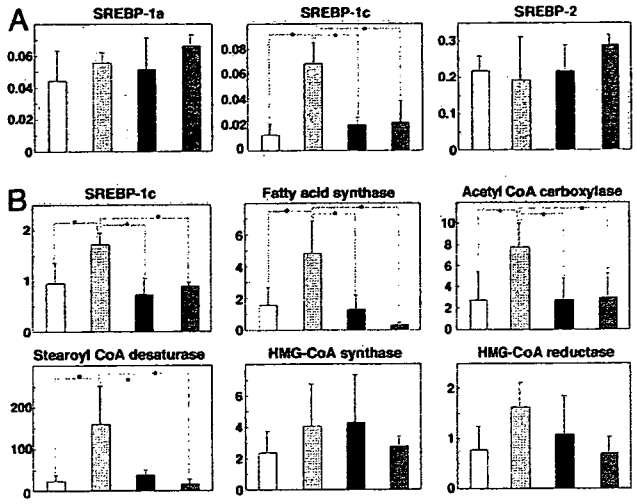

Fig. 3. Transcription of genes regulating lipid biosynthesis in the mouse liver. (*A*) Total RNA was prepared from the livers of 2-month-old mice; and the transcription of genes encoding SREBP-1a, SREBP-1c, and SREBP-2 was determined by real-time PCR. (*B*) The transcription of genes encoding SREBP-1c, fatty acid synthase, acetyl-CoA carboxylase, stearoyl-CoA desaturase, HMG-CoA synthase, and HMG-CoA reductase of 6-month-old mice was measured by real-time PCR. The transcription of the genes was normalized with that of hypoxanthine phosphoribosyltransferase, and the values are expressed as relative activity ($n = 5$; *, $P < 0.05$; **, $P < 0.01$). The transcription of each gene in PA28$\gamma^{+/+}$, PA28$\gamma^{+/+}$CoreTg, PA28$\gamma^{-/-}$CoreTg, and PA28$\gamma^{-/-}$ mice is indicated by white, gray, black, and dark gray bars, respectively.

metabolism, genes related to the lipid biosyntheses were examined by real-time quantitative PCR. Transcription of SREBP-1c was higher in the livers of PA28$\gamma^{+/+}$CoreTg mice than in those of PA28$\gamma^{+/+}$, PA28$\gamma^{-/-}$, and PA28$\gamma^{-/-}$CoreTg mice at 2 months of age, but no such increases in SREBP-2 and SREBP-1a were observed (Fig. 3*A*). Although transcription of SREBP-1c and its regulating enzymes, such as acetyl-CoA carboxylase, fatty acid synthase, and stearoyl-CoA desaturase, was also enhanced in the livers of 6-month-old PA28$\gamma^{+/+}$CoreTg mice compared with the levels in the livers of PA28$\gamma^{+/+}$, PA28$\gamma^{-/-}$, and PA28$\gamma^{-/-}$CoreTg mice, no statistically significant differences were observed with respect to the transcription levels of cholesterol biosynthesis-related genes that are regulated by SREBP-2 (e.g., HMG-CoA synthase and HMG-CoA reductase) (Fig. 3*B*). These results suggest the following: (*i*) the up-regulation of SREBP-1c transcription in the livers of mice requires both HCV core protein and PA28γ; and (*ii*) the nuclear accumulation of HCV core protein alone, which occurs because of the lack of degradation along a PA28γ-dependent proteasome pathway, does not activate the *srebp-1c* promoter.

HCV Core Protein Indirectly Potentiates *srebp-1c* Promoter Activity in an LXRα/RXRα-Dependent Manner. LXRα, which is primarily expressed in the liver, forms a complex with RXRα and synergistically potentiates *srebp-1c* promoter activity (16). Activation of RXRα by HCV core protein suggests that cellular fatty acid synthesis is modulated by the SREBP-1c pathway, although HCV core protein was not included in the transcription factor complex in the electrophoresis mobility shift assay (EMSA) (17). To analyze the effect of HCV core protein and PA28γ on the activation of the *srebp-1c* promoter, we first examined the effect of HCV core protein on the binding of the LXRα/RXRα complex to the LXR-response element (LXRE) located upstream of the SREBP-1c gene (Fig. 4*A*). Although a weak shift of the labeled LXRE probe was observed by incubation with nuclear extracts prepared from 293T cells expressing FLAG-tagged LXRα and HA-tagged RXRα, a clear shift was obtained by the treatment of cells with 9-*cis*-retinoic acid and 22(*R*)-hydroxylcholesterol, ligands for LXRα and RXRα, respectively. In contrast, coexpression of HCV core protein with LXRα and RXRα potentiated the shift of the probe irrespective of the treatment with the ligands. Addition of 500 times the amount of nonlabeled LXRE probe (competitor) diminished the shift of the labeled probe induced by the ligands and/or HCV core protein. Furthermore, coincubation of the nuclear fraction with antibody to FLAG or HA tag but not with antibody to either HCV core or PA28γ caused a supershift of the labeled probe. These results indicate that HCV core protein does not participate in the LXRα/RXRα–LXRE complex but indirectly enhances the binding of LXRα/RXRα to the LXRE.

The activity of the *srebp-1c* promoter was enhanced by the expression of HCV core protein in 293T cells, and it was further enhanced by coexpression of LXRα/RXRα (Fig. 4*B*). Enhancement of the *srebp-1c* promoter by coexpression of HCV core protein and LXRα/RXRα was further potentiated by treatment with the ligands for LXRα and RXRα. The cells treated with 9-*cis*-retinoic acid exhibited more potent enhancement of the *srebp-1c* promoter than those treated with 22(*R*)-hydroxylcholesterol. HCV core protein exhibited more potent enhancement of the *srebp-1c* promoter in cells treated with both ligands than in those treated with either ligand alone. These results suggest that HCV core protein poten-

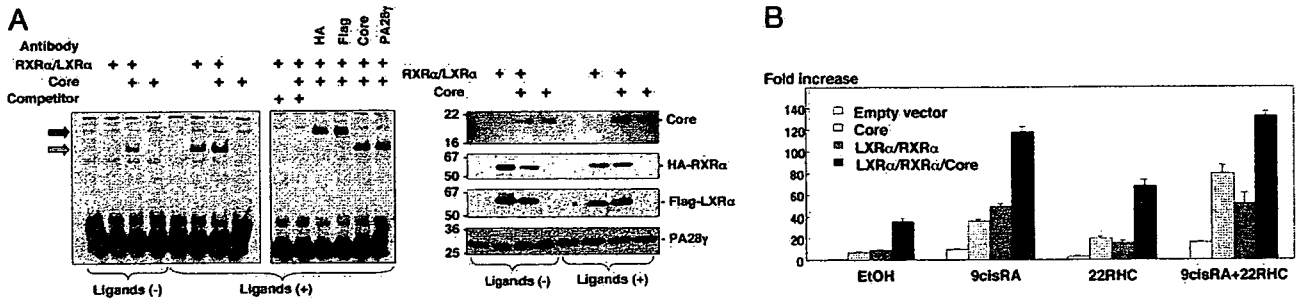

Fig. 4. Activation of the *srebp-1c* promoter by HCV core protein. (*A*) FLAG-LXRα and HA-RXRα were expressed in 293T cells together with or without HCV core protein. Ligands for LXRα and RXRα dissolved in ethanol [Ligands (+)] or ethanol alone [Ligands (−)] were added to the culture supernatant at 24 h posttransfection. Cells were harvested at 48 h posttransfection, and nuclear extracts were mixed with the reaction buffer for EMSA in the presence or absence of antibody (100 ng) against HA, FLAG, HCV core or PA28γ, or nonlabeled LXRE probe (Competitor). (*Left*) The resulting mixtures were subjected to PAGE and blotted with horseradish peroxidase/streptavidin. The mobility shift of the LXRE probe and its supershift are indicated by a gray and black arrow, respectively. (*Right*) Expression of HCV core, HA-RXRα, FLAG-LXRα, and PA28γ in cells was detected by immunoblotting. (*B*) Effects of ligands for RXRα, 9-*cis*-retinoic acid (9cisRA), and for LXRα, 22(*R*)-hydroxylcholesterol (22RHC), on the activation of the *srebp-1c* promoter in 293T cells expressing RXRα, LXRα, and/or HCV core protein. Ligands were added into the medium at 24 h posttransfection at a concentration of 5 μM, and the cells were harvested after 24 h of incubation.

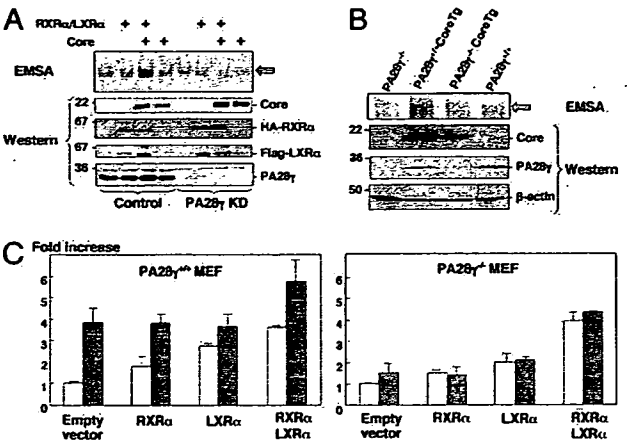

Fig. 5. PA28γ is required for HCV core-dependent activation of the *srebp-1c* promoter. (*A*) Effect of PA28γ knockdown on the LXRα/RXRα–DNA complex. FLAG-LXRα and HA-RXRα were expressed in FLC4 (control) or PA28γ-knockdown (PA28γ KD) cells together with or without HCV core protein. Cells were harvested at 48 h posttransfection, and nuclear extracts were mixed with the reaction buffer for EMSA. (*Upper*) The resulting mixtures were subjected to PAGE and blotted with horseradish peroxidase-streptavidin. The mobility shift of the LXRE probe is indicated by an arrow. (*Lower*) Expression of HCV core, HA-RXRα, FLAG-LXRα, and PA28γ in cells was detected by immunoblotting. (*B*) Effect of PA28γ knockout on the LXRα/RXRα–DNA complex in the mouse liver. (*Upper*) Nuclear extracts were prepared from the livers of 2-month-old PA28γ$^{-/-}$, PA28γ$^{+/+}$CoreTg, PA28γ$^{-/-}$CoreTg, and PA28γ$^{+/+}$ mice and subjected to EMSA. The mobility shift of the LXRE probe is indicated by an arrow. (*Lower*) The expression of HCV core, PA28γ, and β-actin in the livers of the mice was detected by immunoblotting. (*C*) Effect of HCV core protein on *srebp-1* promoter activity in PA28γ-knockout fibroblasts. A plasmid encoding firefly luciferase under the control of the *srebp-1c* promoter was transfected into MEFs prepared from PA28γ$^{+/+}$ (*Left*) or PA28γ$^{-/-}$ (*Right*) mice together with a plasmid encoding a *Renilla* luciferase. An empty plasmid or plasmids encoding mouse RXRα or LXRα were also cotransfected into the cells together with (gray bars) or without (white bars) a plasmid encoding HCV core protein. Luciferase activity under the control of the *srebp-1c* promoter was determined, and it is expressed as the fold increase in relative luciferase activity after standardization with the activity of *Renilla* luciferase.

tiates *srebp-1c* promoter activity in an LXRα/RXRα-dependent manner.

HCV Core Protein Activates the *srepb-1c* Promoter in an LXRα/RXRα- and PA28γ-Dependent Manner. To examine whether PA28γ is required for HCV core-induced enhancement of *srebp-1c* promoter activity in human liver cells, a PA28γ-knockdown human hepatoma cell line (FLC4 KD) was prepared. Enhancement of binding of the LXRE probe to LXRα/RXRα by coexpression of HCV core protein and LXRα/RXRα in FLC4 cells was diminished by knockdown of the PA28γ gene (Fig. 5*A*). Furthermore, formation of the LXRα/RXRα–LXRE complex was enhanced in the livers of PA28γ$^{+/+}$CoreTg mice but not in those of PA28γ$^{-/-}$, PA28γ$^{+/+}$, or PA28γ$^{-/-}$CoreTg mice (Fig. 5*B*). The expression of the HCV core protein in the mouse embryonic fibroblasts (MEFs) of PA28γ$^{+/+}$ mice induced the activation of the mouse *srebp-1c* promoter through the endogenous expression of LXRα and RXRα (Fig. 5*C Left*). Further enhancement of the activation of the *srebp-1c* promoter by HCV core protein in PA28γ$^{+/+}$ MEFs was achieved by the exogenous expression of both LXRα and RXRα. However, no enhancing effect of HCV core protein on *srebp-1c* promoter activity was observed in PA28γ$^{-/-}$ MEFs (Fig. 5*C Right*). These results support the notion that HCV core protein enhances the activity of the *srepb-1c* promoter in an LXRα/RXRα- and PA28γ-dependent manner.

Table 1. HCC in mice at 16–18 months of age

Mouse and sex	Total no. of mice	No. of mice developing HCC	Incidence, %
PA28γ$^{+/+}$CoreTg			
Male	17	5	29.4
Female	28	3	10.7
PA28γ$^{+/-}$			
Male	16	0	0
Female	4	0	0
PA28γ$^{-/-}$			
Male	23	0	0
Female	13	0	0
PA28γ$^{-/-}$CoreTg			
Male	15	0	0
Female	21	0	0

PA28γ Plays a Crucial Role in the Development of HCC in PA28γ$^{+/+}$ CoreTg Mice. The incidence of hepatic tumors in male PA28γ$^{+/+}$ CoreTg mice older than 16 months was significantly higher than that in age-matched female PA28γ$^{+/+}$CoreTg mice (6). We reconfirmed here that the incidence of HCC in male and female PA28γ$^{+/+}$CoreTg mice at 16–18 months of age was 29.4% (5 of 17 mice) and 10.7% (3 of 28 mice), respectively. To our surprise, however, no HCC developed in PA28γ$^{-/-}$CoreTg mice (males, 15; females, 21), although, as expected, no HCC was observed in PA28γ$^{+/-}$ (males, 16; females, 4) and PA28γ$^{-/-}$ mice (males, 23; females, 13) (Table 1). These results clearly indicate that PA28γ plays an indispensable role in the development of HCC induced by HCV core protein.

Discussion

HCV core protein is detected in the cytoplasm and partially in the nucleus and mitochondria of culture cells and hepatocytes of transgenic mice and hepatitis C patients (6, 23, 24, 26). Degradation of HCV core protein was enhanced by deletion of the C-terminal transmembrane region through a ubiquitin/proteasome-dependent pathway (27). We previously reported (18) that PA28γ binds directly to HCV core protein and then enhances degradation of HCV core protein in the nucleus through a proteasome-dependent pathway because HCV core protein was accumulated in nucleus of human cell line by treatment with proteasome inhibitor MG132. In this work, accumulation of HCV core protein was observed in nucleus of hepatocytes of PA28γ$^{-/-}$CoreTg mice (Fig. 1*D*). This result directly demonstrates that HCV core protein migrates into the nucleus and is degraded through a PA28γ-dependent pathway. However, HCV core protein accumulated in the nucleus because knockout of PA28γ gene abrogated the ability to cause liver pathology, suggesting that interaction of HCV core protein with PA28γ in the nucleus is prerequisite for the liver pathology induced by HCV core protein. We have previously shown (18) that HCV core protein is degraded through a PA28γ-dependent pathway, and Minami *et al.* (28) reported that PA28γ has a cochaperone activity with Hsp90. Therefore, degradation products of HCV core protein by means of PA28γ-dependent processing or correct folding of HCV core protein through cochaperone activity of PA28γ might be involved in the development of liver pathology. We do not know the reason why knockout of the PA28γ gene does not affect the total amount of HCV core protein in the liver of the transgenic mice. PA28γ-dependent degradation of HCV core protein may be independent of ubiquitination, as shown in SRC-3 (21), whereas knockdown of PA28γ in a human hepatoma cell line enhanced the ubiquitination of HCV core protein [supporting information (SI) Fig. 6], suggesting that lack of PA28γ suppresses a ubiquitin-independent degradation but enhances a ubiquitin-dependent degradation of HCV core protein. Therefore, the total amount of HCV

core protein in the liver of the mice may be unaffected by the knockout of the PA28γ gene.

Our results suggest that the interaction of HCV core protein with PA28γ leads to the activation of the *srebp-1c* promoter along an LXRα/RXRα-dependent pathway and the development of liver steatosis and HCC. HCV core protein was not included in the LXRα/RXRα–LXRE complex (Fig. 3*A*), suggesting that HCV core protein indirectly activates the *srebp-1c* promoter. Cytoplasmic HCV core protein was shown to interact with Sp110b, which is a transcriptional corepressor of RARα-dependent transcription, and this interaction leads to the sequestering of Sp110b in the cytoplasm, resulting in the activation of RARα-dependent transcription (29). The sequestration of an unidentified corepressor of the LXRα/RXRα heterodimer in the cytoplasm by HCV core protein may also contribute to the activation of the *srebp-1c* promoter. Although the precise physiological function of PA28γ-proteasome activity in the nucleus is not known, PA28γ has previously been shown (21) to regulate nuclear hormone receptors by means of the degradation of its coactivator SRC-3 and to participate in the fully Hsp90-dependent protein refolding (28). It appears reasonable to speculate that degradation or refolding of HCV core protein in a PA28γ-dependent pathway might be involved in the modulation of transcriptional regulators of various promoters, including the *srebp-1c* promoter. Saturated or monounsaturated fatty acids have been shown to enhance HCV RNA replication in Huh7 cells containing the full-length HCV replicon (7). The up-regulation of fatty acid biosynthesis by HCV core protein may also contribute to the efficient replication of HCV and to the progression of HCV pathogenesis.

Expression of HCV core protein was reported to enhance production of reactive oxygen species (ROS) (30), which leads to carbonylation of intracellular proteins (31). Enhancement of ROS production may trigger double-stranded DNA breaks and result in the development of HCC (30, 32, 33). HCV core protein could enhance the protein carbonylation in the liver of the transgenic mice in the presence but not in the absence of PA28γ (SI Fig. 7), suggesting that PA28γ is required for ROS production induced by HCV core protein. Development of HCC was observed in PA28γ$^{+/+}$CoreTg mice but not in PA28γ$^{-/-}$CoreTg mice (Table 1). Enhancement of ROS production by HCV core protein in the presence of PA28γ might be involved in the development of HCC in PA28γ$^{+/+}$CoreTg mice.

It is well known that resistant viruses readily emerge during the treatment with antiviral drugs targeting the viral protease or replicase, especially in the case of infection with RNA viruses. Therefore, antivirals targeting the host factors that are indispensable for the propagation of viruses might be an ideal target for the development of antiviral agents because of a lower rate of mutation than that of viral genome, if they have no side effects to patients. Importantly, the amino acid sequence of PA28γ of mice is identical to that of human, and mouse PA28γ is dispensable because PA28γ knockout mice exhibit no abnormal phenotype except for mild growth retardation. Therefore, PA28γ might be a promising target for an antiviral treatment of chronic hepatitis C with negligible side effects.

In summary, we observed that a knockout of the PA28γ gene from PA28γ$^{+/+}$CoreTg mice induced the accumulation of HCV core protein in the nucleus and disrupted the development of both steatosis and HCC. Activation of the *srebp-1c* promoter was up-regulated by HCV core protein both *in vitro* and *in vivo* through a PA28γ-dependent pathway, suggesting that PA28γ plays a crucial role in the development of liver pathology induced by HCV infection.

Materials and Methods

Histology and immunohistochemistry, real-time PCR, and detection of proteins modified by ROS are discussed in *SI Materials and Methods*.

Plasmids and Reagents. Human PA28γ cDNA was isolated from a human fetal brain library (18). The gene encoding HCV core protein was amplified from HCV strain J1 (genotype 1b) (34) and cloned into pCAG-GS (35). Mouse cDNAs of RXRα and LXRα were amplified by PCR from the total cDNAs of the mouse liver. The RXRα and LXRα genes were introduced into pEF-FLAGGspGBK (36) and pcDNA3.1 (Invitrogen, Carlsbad, CA), respectively. The targeting fragment for human PA28γ knockdown (GGATCCGGTGGATCAGGAAGTGAAGTTCAAGAGA-CTTCACTTCCTGATCCACCTTTTTTGGAAAAGCTT) was introduced into the BamHI and HindIII sites of pSilencer 4.1 U6 hygro vector (Ambion, Austin, TX). Mouse anti-FLAG (M2) and mouse anti-β-actin antibodies were purchased from Sigma (St. Louis, MO). Rabbit polyclonal antibody against synthetic peptides corresponding to amino acids 70–85 of PA28γ was obtained from AFFINITI (Exeter, U.K.). Horseradish peroxidase-conjugated goat anti-mouse and anti-rabbit IgGs were purchased from ICN Pharmaceuticals (Aurora, OH). Rabbit anti-HCV core protein was prepared by immunization with recombinant HCV core protein (amino acids 1-71), as described in ref. 24. Mouse monoclonal antibody to HCV core protein was kindly provided by S. Yagi (37). The plasmid for expression of HA-tagged ubiquitin was described in ref. 27.

Preparation of PA28γ-Knockout HCV CoreTg Mice. The generation of C57BL/6 mice carrying the gene encoding HCV core protein genotype 1b line C49 and that of PA28γ$^{-/-}$ mice have been reported previously (22, 25). Both strains were crossbred with each other to create PA28γ$^{-/-}$CoreTg mice. PA28γ$^{-/-}$CoreTg mice were identified by PCR targeted at the PA28γ or HCV core gene (22, 25). Using 1 μg of genomic DNA obtained from the mouse tail, the PA28γ gene was amplified by PCR with the following primers: sense, PA28-3 (AGGTGGATCAGGAAGTGAAGCTCAA); and antisense, PA28γ-5cr (CACCTCACTTGTGATCCGCTCTCT-GAAAGAATCAACC). The targeted sequence for the PA28γ-knockout mouse was detected by PCR using the PA28-3 primer and the PAKO-4 primer (TGCAGTTCATTCAGGGCACCGGA-CAG). The transgene encoding HCV core protein was detected by PCR as described in ref. 25. The expression of PA28γ and HCV core protein in the livers of 6-month-old mice was confirmed by Western blotting with mouse monoclonal antibody to HCV core protein, clone 11-10, and rabbit antibody to PA28γ. Mice were cared for according to the institutional guidelines. The mice were given ordinary feed, CRF-1 (Charles River Laboratories, Yokohama, Japan), and they were maintained under specific pathogen-free conditions.

All animal experiments conformed to the Guidelines for the Care and Use of Laboratory Animals, and they were approved by the Institutional Committee of Laboratory Animal Experimentation (Research Institute for Microbial Diseases, Osaka University).

Preparation of Mouse Embryonic Fibroblasts. MEFs were prepared as described in ref. 22. MEFs were cultured at 37°C under an atmosphere of 5% CO_2 in Dulbecco's modified Eagle's medium (Sigma) supplemented with 10% FBS, penicillin, streptomycin, sodium pyruvate, and nonessential amino acids.

Transfection and Immunoblotting. Plasmid vectors were transfected into the MEFs and 293T cells by liposome-mediated transfection by using Lipofectamine 2000 (Invitrogen). The amount of HCV core protein in the liver tissues was determined by an ELISA as described in ref. 37. The cell lysates were subjected to SDS/PAGE (12.5% gel), and they were then transferred onto PVDF membranes. Proteins on the membranes were treated with specific antibody and Super Signal Femto (Pierce, Rockford, IL). The results were then visualized by using an LAS3000 imaging system (Fuji Photo Film, Tokyo, Japan). The method of immunoprecipitation test is described in ref. 18.

Reporter Assay for *srebp-1c* Promoter Activity. The genomic DNA fragment encoding the *srebp-1c* promoter region (located from residues −410 to +24) was amplified from a mouse genome. The fragment was introduced into the KpnI and HindIII sites of pGL3-Basic (Promega, Madison, WI), and it was designated as pGL3-srebp-1cPro. The plasmids encoding RXRα and LXRα were transfected into MEFs together with pGL3-srebp-1cPro and a control plasmid encoding *Renilla* luciferase (Promega). The total DNA for transfection was normalized by the addition of empty plasmids. Cells were harvested at 24 h posttransfection. The ligand of RXRα, 9-*cis*-retinoic acid (Sigma), and that of LXRα, 22(*R*)-hydroxylcholesterol (Sigma) were added at a final concentration of 5 μM each to the culture medium of 293T cells transfected with pGL3-srebp-1cPro together with expression plasmids encoding RXRα, LXRα, and HCV core protein at 24 h posttransfection. Cells were harvested 24 h after treatment. Luciferase activity was measured by using the dual-luciferase reporter assay system (Promega). Firefly luciferase activity was standardized with that of *Renilla* luciferase, and the results are expressed as the fold increase in relative luciferase units.

Electrophoresis Mobility Shift Assay (EMSA). EMSA was carried out by using a LightShift Chemiluminescent EMSA kit (Pierce) according to the manufacturer's protocol. Nuclear extract of the cell lines and liver tissue was prepared with an NE-PER nuclear and cytoplasmic extraction reagent kit (Pierce). Briefly, double-stranded oligonucleotides for EMSA were prepared by annealing both strands of each LXRE of the *srebp-1c* promoter (5′-GGACGCCCGCTAGTAACCCCGGC-3′) (16). Both strands were labeled at the 5′ ends with biotin. The annealed probe was incubated for 20 min on ice with nuclear extract (3 μg of protein) in a reaction buffer containing 10 mM Tris·HCl (pH 7.5), 50 mM KCl, 1 mM DTT, 0.05 μg/μl poly(dI-dC), 2.5% glycerol, 0.05% Nonidet P-40, and 0.1 nM labeled probe, with or without 1 mM nonlabeled probe. The resulting mixture was subjected to PAGE (5% gel) at 120 V for 30 min in 0.5× TBE. The DNA–protein complex was transferred to a Hybond N+ membrane (Amersham, Piscataway, NJ), incubated with horseradish peroxidase-conjugated streptavidin, and visualized by using an LAS3000 imaging system.

Statistical Analysis. The results are expressed as the mean ± SD. The significance of differences in the means was determined by Student's *t* test.

We thank H. Murase for secretarial work and D. C. S. Huang for providing the plasmids. This work was supported in part by grants-in-aid from the Ministry of Health, Labor, and Welfare; the Ministry of Education, Culture, Sports, Science, and Technology; the 21st Century Center of Excellence Program; and the Foundation for Biomedical Research and Innovation.

1. Wasley A, Alter MJ (2000) *Semin Liver Dis* 20:1–16.
2. Bach N, Thung SN, Schaffner F (1992) *Hepatology* 15:572–577.
3. Lefkowitch JH, Schiff ER, Davis GL, Perrillo RP, Lindsay K, Bodenheimer HC, Jr., Balart LA, Ortego TJ, Payne J, Dienstag JL, *et al.* (1993) *Gastroenterology* 104:595–603.
4. Barba G, Harper F, Harada T, Kohara M, Goulinet S, Matsuura Y, Eder G, Schaff Z, Chapman MJ, Miyamura T, Brechot C (1997) *Proc Natl Acad Sci USA* 94:1200–1205.
5. Hope RG, McLauchlan J (2000) *J Gen Virol* 81:1913–1925.
6. Moriya K, Fujie H, Shintani Y, Yotsuyanagi H, Tsutsumi T, Ishibashi K, Matsuura Y, Kimura S, Miyamura T, Koike K (1998) *Nat Med* 4:1065–1067.
7. Kapadia SB, Chisari FV (2005) *Proc Natl Acad Sci USA* 102:2561–2566.
8. Su AI, Pezacki JP, Wodicka L, Brideau AD, Supekova L, Thimme R, Wieland S, Bukh J, Purcell RH, Schultz PG, Chisari FV (2002) *Proc Natl Acad Sci USA* 99:15669–15674.
9. Wang C, Gale M, Jr, Keller BC, Huang H, Brown MS, Goldstein JL, Ye J (2005) *Mol Cell* 18:425–434.
10. Horton JD, Shimomura I, Brown MS, Hammer RE, Goldstein JL, Shimano H (1998) *J Clin Invest* 101:2331–2339.
11. Pai JT, Guryev O, Brown MS, Goldstein JL (1998) *J Biol Chem* 273:26138–26148.
12. Shimano H, Horton JD, Hammer RE, Shimomura I, Brown MS, Goldstein JL (1996) *J Clin Invest* 98:1575–1584.
13. Shimano H, Horton JD, Shimomura I, Hammer RE, Brown MS, Goldstein JL (1997) *J Clin Invest* 99:846–854.
14. Shimano H, Shimomura I, Hammer RE, Herz J, Goldstein JL, Brown MS, Horton JD (1997) *J Clin Invest* 100:2115–2124.
15. Repa JJ, Liang G, Ou J, Bashmakov Y, Lobaccaro JM, Shimomura I, Shan B, Brown MS, Goldstein JL, Mangelsdorf DJ (2000) *Genes Dev* 14:2819–2830.
16. Yoshikawa T, Shimano H, Amemiya-Kudo M, Yahagi N, Hasty AH, Matsuzaka T, Okazaki H, Tamura Y, Iizuka Y, Ohashi K, *et al.* (2001) *Mol Cell Biol* 21:2991–3000.
17. Tsutsumi T, Suzuki T, Shimoike T, Suzuki R, Moriya K, Shintani Y, Fujie H, Matsuura Y, Koike K, Miyamura T (2002) *Hepatology* 35:937–946.
18. Moriishi K, Okabayashi T, Nakai K, Moriya K, Koike K, Murata S, Chiba T, Tanaka K, Suzuki R, Suzuki T, *et al.* (2003) *J Virol* 77:10237–10249.
19. Masson P, Andersson O, Petersen UM, Young P (2001) *J Biol Chem* 276:1383–1390.
20. Li J, Rechsteiner M (2001) *Biochimie* 83:373–383.
21. Li X, Lonard D, Jung SY, Malovannaya A, Feng Q, Qin J, Tsai SY, Tsai M, O'Malley BW (2006) *Cell* 124:381–392.
22. Murata S, Kawahara H, Tohma S, Yamamoto K, Kasahara M, Nabeshima Y, Tanaka K, Chiba T (1999) *J Biol Chem* 274:38211–38215.
23. Falcon V, Acosta-Rivero N, Chinea G, Gavilondo J, de la Rosa MC, Menendez I, Duenas-Carrera S, Vina A, Garcia W, Gra B, *et al.* (2003) *Biochem Biophys Res Commun* 305:1085–1090.
24. Suzuki R, Sakamoto S, Tsutsumi T, Rikimaru A, Tanaka K, Shimoike T, Moriishi K, Iwasaki T, Mizumoto K, Matsuura Y, *et al.* (2005) *J Virol* 79:1271–1281.
25. Moriya K, Yotsuyanagi H, Shintani Y, Fujie H, Ishibashi K, Matsuura Y, Miyamura T, Koike K (1997) *J Gen Virol* 78:1527–1531.
26. Yasui K, Wakita T, Tsukiyama-Kohara K, Funahashi SI, Ichikawa M, Kajita T, Moradpour D, Wands JR, Kohara M (1998) *J Virol* 72:6048–6055.
27. Suzuki R, Tamura K, Li J, Ishii K, Matsuura Y, Miyamura T, Suzuki T (2001) *Virology* 280:301–309.
28. Minami Y, Kawasaki H, Minami M, Tanahashi N, Tanaka K, Yahara I (2000) *J Biol Chem* 275:9055–9061.
29. Watashi K, Hijikata M, Tagawa A, Doi T, Marusawa H, Shimotohno K (2003) *Mol Cell Biol* 23:7498–7509.
30. Machida K, Cheng KT, Lai CK, Jeng KS, Sung VM, Lai MM (2006) *J Virol* 80:7199–7207.
31. Nystrom T (2005) *EMBO J* 24:1311–1317.
32. Bromberg JF, Wrzeszczynska MH, Devgan G, Zhao Y, Pestell RG, Albanese C, Darnell JE, Jr (1999) *Cell* 98:295–303.
33. Carballo M, Conde M, El Bekay R, Martin-Nieto J, Camacho MJ, Monteseirin J, Conde J, Bedoya FJ, Sobrino F (1999) *J Biol Chem* 274:17580–17586.
34. Aizaki H, Aoki Y, Harada T, Ishii K, Suzuki T, Nagamori S, Toda G, Matsuura Y, Miyamura T (1998) *Hepatology* 27:621–627.
35. Niwa H, Yamamura K, Miyazaki J (1991) *Gene* 108:193–199.
36. Huang DC, Cory S, Strasser A (1997) *Oncogene* 14:405–414.
37. Aoyagi K, Ohue C, Iida K, Kimura T, Tanaka E, Kiyosawa K, Yagi S (1999) *J Clin Microbiol* 37:1802–1808.

JOURNAL OF VIROLOGY, Feb. 2007, p. 1727–1735 Vol. 81, No. 4
0022-538X/07/$08.00+0 doi:10.1128/JVI.01683-06

Involvement of the PA28γ-Dependent Pathway in Insulin Resistance Induced by Hepatitis C Virus Core Protein▽

Hironobu Miyamoto,[1] Kohji Moriishi,[1] Kyoji Moriya,[2] Shigeo Murata,[3] Keiji Tanaka,[3] Tetsuro Suzuki,[4] Tatsuo Miyamura,[4] Kazuhiko Koike,[2] and Yoshiharu Matsuura[1]*

Department of Molecular Virology, Research Institute for Microbial Diseases, Osaka University, Osaka,[1] Department of Internal Medicine, Graduate School of Medicine, University of Tokyo, Tokyo,[2] Department of Molecular Oncology, Tokyo Metropolitan Institute of Medical Science, Tokyo,[3] and Department of Virology II, National Institute of Infectious Diseases, Tokyo,[4] Japan

Received 4 August 2006/Accepted 16 November 2006

The hepatitis C virus (HCV) core protein is a component of nucleocapsids and a pathogenic factor for hepatitis C. Several epidemiological and experimental studies have suggested that HCV infection is associated with insulin resistance, leading to type 2 diabetes. We have previously reported that HCV core gene-transgenic (PA28γ$^{+/+}$CoreTg) mice develop marked insulin resistance and that the HCV core protein is degraded in the nucleus through a PA28γ-dependent pathway. In this study, we examined whether PA28γ is required for HCV core-induced insulin resistance in vivo. HCV core gene-transgenic mice lacking the PA28γ gene (PA28γ$^{-/-}$CoreTg) were prepared by mating of PA28γ$^{+/+}$CoreTg with PA28γ-knockout mice. Although there was no significant difference in the glucose tolerance test results among the mice, the insulin sensitivity in PA28γ$^{-/-}$CoreTg mice was recovered to a normal level in the insulin tolerance test. Tyrosine phosphorylation of insulin receptor substrate 1 (IRS1), production of IRS2, and phosphorylation of Akt were suppressed in the livers of PA28γ$^{+/+}$CoreTg mice in response to insulin stimulation, whereas they were restored in the livers of PA28γ$^{-/-}$CoreTg mice. Furthermore, activation of the tumor necrosis factor alpha promoter in human liver cell lines or mice by the HCV core protein was suppressed by the knockdown or knockout of the PA28γ gene. These results suggest that the HCV core protein suppresses insulin signaling through a PA28γ-dependent pathway.

Hepatitis C virus (HCV) is the causative agent in most cases of acute and chronic non-A, non-B hepatitis (15). Over one-half of patients with the acute infection evolve into a persistent carrier state (24). Chronic infection with HCV frequently induces hepatic steatosis, cirrhosis, and eventually hepatocellular carcinoma (22) and is known to be associated with diseases of extrahepatic organs, including an essential mixed cryoglobulinemia, porphyria cutanea tarda, membranoproliferative glomerulonephritis, and type 2 diabetes (13).

HCV is classified into the genus *Hepacivirus* of the family *Flaviviridae* and possesses a viral genome consisting of a single positive-strand RNA with a nucleotide length of about 9.5 kb. This viral genome encodes a single polyprotein composed of approximately 3,000 amino acids (9). The polyprotein is post-translationally cleaved by host cellular peptidases and viral proteases, resulting in 10 viral proteins (6, 10, 12). The HCV core protein is known to interact with viral-sense RNA of HCV to form the viral nucleocapsid (44). The HCV core protein is cleaved off at residue 191 by the host signal peptidase to release it from the E1 envelope protein and then by the host signal peptide peptidase at around amino acid residues 177 to 179 within the C-terminal transmembrane region (30, 39, 40). The mature core protein is retained mainly on the endoplasmic reticulum, although a portion moves to the nucleus and mitochondria (11, 51).

Recent epidemiological studies have indicated that type 2 diabetes is an HCV-associated disease (7, 29). However, it remains unclear how insulin resistance is induced in patients chronically infected with HCV, since there is no suitable model for investigating HCV pathogenesis. Type 2 diabetes is a complex, multisystemic disease with pathophysiology that includes a high level of hepatic glucose production and insulin resistance, which contribute to the development of hyperglycemia (8, 18). Although the precise mechanism by which these factors contribute to the induction of insulin resistance is difficult to understand, a high level of insulin production by pancreatic β cells under a state of insulin resistance is common in the development of type 2 diabetes. The hyperinsulinemia in the fasting state that is observed relatively early in type 2 diabetes is considered to be a secondary response that compensates for the insulin resistance (8, 18).

The HCV core protein is also known as a pathogenic factor that induces steatosis and hepatocellular carcinoma in mice (33, 35). Previously, we reported that insulin resistance occurs in HCV core gene-transgenic mice due at least partly to an increase in tumor necrosis factor alpha (TNF-α) secretion (47) and that the HCV core protein is degraded through a PA28γ/REGγ (11S regulator)-dependent pathway in the nucleus (32). It is well known that PA28γ enhances latent proteasome activity, although the biological significance of PA28γ is largely unknown, with the exception that PA28γ is known to regulate steroid receptor coactivator 3 (28). Although several reports suggested that the degradation of insulin receptor substrate (IRS) proteins by a ubiquitin-dependent proteasome activity contributes to insulin resistance (43, 50), the involvement of the HCV core protein in cooperation with PA28γ in the stability of IRS proteins and in the development of insulin resis-

* Corresponding author. Mailing address: Department of Molecular Virology, Research Institute for Microbial Diseases, Osaka University, 3-1 Yamadaoka, Suita, Osaka 565-0871, Japan. Phone: 81-6-6879-8340. Fax: 81-6-6879-8269. E-mail: matsuura@biken.osaka-u.ac.jp.

▽ Published ahead of print on 29 November 2006.

tance is not known. In this study, we examined the involvement of PA28γ in the induction of insulin resistance by the HCV core protein in vivo.

MATERIALS AND METHODS

Preparation of PA28γ-knockout HCV core gene-transgenic mice. C57BL/6 mice carrying the gene encoding HCV core protein genotype 1b (PA28γ$^{+/+}$ CoreTg) line C49 and PA28γ$^{-/-}$ mice have been described previously (35, 36). These two genotypes were crossbred to create PA28γ$^{+/-}$CoreTg mice. PA28γ$^{+/-}$CoreTg mice were bred to generate PA28γ$^{-/-}$CoreTg mice (35, 36). The HCV core gene and the target sequence to knock out the PA28γ gene were identified by PCR. The mice were given ordinary feed (CRF-1; Charles River Laboratories, Yokohama, Japan) and were maintained under specific-pathogen-free conditions.

Glucose tolerance test. The mice were fasted for more than 16 h before glucose administration. D-Glucose (1 g/kg body weight) was intraperitoneally administered to the mice. Blood samples were taken from the orbital sinus at the indicated time points. The plasma glucose concentration was measured by means of a MEDI-SAFE Mini blood glucose monitor (TERUMO, Tokyo, Japan). The serum insulin level was determined by a Mercodia (Uppsala, Sweden) ultrasensitive mouse insulin enzyme-linked immunosorbent assay (ELISA).

Insulin tolerance test. The mice were fed freely and then fasted during the study period. Human insulin (2 U/kg body weight) (Humulin; Eli Lilly, Indianapolis, IN) was intraperitoneally administered to the mice. The plasma glucose concentration was measured at the indicated time and was normalized based on the glucose concentration at the time just before insulin administration.

Histological analysis of pancreatic islets. Pancreas tissues were fixed with paraformaldehyde, embedded in paraffin, sectioned, and stained with hematoxylin and eosin. The relative islet area and islet number were determined with Image-Pro PLUS image analyzing software (NIPPON ROPER, Tokyo, Japan).

Estimation of tumor necrosis factor alpha and HCV core protein. Mouse TNF-α was measured by using a mouse TNF-α ELISA kit (Pierce, Rockford, IL) and normalized based on the amount of total protein in each sample. The protein concentration was estimated by using a BCA protein assay kit (Pierce). The amount of HCV core protein in the liver tissues was determined by using an ELISA system as described previously (4).

In vivo insulin stimulation and immunoblot analysis. Mice were fasted for more than 16 h before insulin stimulation and then anesthetized with ketamine and xylazine. Five units of insulin were injected into the mice via the interior vena cava. Livers of the mice were collected 5 min after the insulin injection and frozen in liquid nitrogen. Immunoblot analyses of the HCV core protein, PA28γ, and each of the insulin-signaling molecules were carried out with the liver tissue homogenates prepared in the homogenizing buffer containing 25 mM Tris-HCl (pH 7.4), 10 mM Na_3VO_4, 100 mM NaF, 50 mM $Na_4P_2O_7$, 10 mM EGTA, 10 mM EDTA, 2 mM phenylmethylsulfonyl fluoride, and 1% Nonidet P40 supplemented with Complete Protease Inhibitor Cocktail (Roche Diagnostics, Mannheim, Germany) (53). Tissue lysates were subjected to sodium dodecyl sulfate–2% to 15% gradient polyacrylamide gel electrophoresis (PAG Mini DAIICHI 2/15 13W; Daiichi Diagnostics, Tokyo, Japan) and electrotransferred onto polyvinylidene difluoride membranes (Immobilon-P; Millipore, Bedford, MA). The protein transferred onto the membrane was reacted with rabbit anti-HCV core (32), rabbit anti-Akt (Cell Signaling, Danvers, MA), rabbit anti-phospho-Ser473-Akt (Cell Signaling), rabbit anti-IRS1 (Upstate, Lake Placid, NY), rabbit anti-phospho-Tyr608 mouse insulin receptor substrate 1 (Sigma, St. Louis, MO), or rabbit anti-IRS2 (Upstate) polyclonal antibody and then incubated with horseradish peroxidase-conjugated anti-rabbit antibody. Blotted protein was visualized using Super Signal Femto (Pierce) and an LAS3000 imaging system (Fuji Photo Film, Tokyo, Japan).

Quantitative reverse transcription-PCR (RT-PCR). Total RNA was isolated from mouse liver using an RNeasy kit (QIAGEN, Valencia, CA). The RNA preparation was treated with a TURBO DNA-free kit (Ambion, Austin, TX) to remove DNA contamination in the samples. The first-strand cDNAs were synthesized by a first-strand cDNA synthesis kit (Amersham Biosciences, Franklin Lakes, NJ). The targeted cDNA was estimated by using Platinum SYBR Green qPCR Super Mix UDC (Invitrogen, Carlsbad, CA) according to the manufacturer's protocol. The fluorescent signal was measured by using an ABI Prism 7000 (Applied Biosystems, Foster City, CA). The genes encoding mouse TNF-α, IRS1, IRS2, and hypoxanthine phosphoribosyl transferase were amplified with the following primer pairs: 5′-GGTACAACCCATCGGCTGGCA-3′ (forward) and 5′-GCGACGTGGAACTGGCAGAAG-3′ (reverse) for TNF-α, 5′-ATAG CTCTGAGACCTTCTCAGCACCTAC-3′ (forward) and 5′-GGAGTTGCCCT CATTGCTGCCTAA-3′ (reverse) for IRS1, 5′-AGCCTGGGGATAATGGTG ACTATACCGA-3′ (forward) and 5′-TTGTGGGCAAAGGATGGGGACAC T-3′ (reverse) for IRS2, and 5′-CCAGCAAGCTTGCAACCTTAACCA-3′ (forward) and 5′-GTAATGATCAGTCAACGGGGGAC-3′ (reverse) for hypoxanthine phosphoribosyl transferase. Each PCR product was found as a single band with the correct size by agarose gel electrophoresis (data not shown).

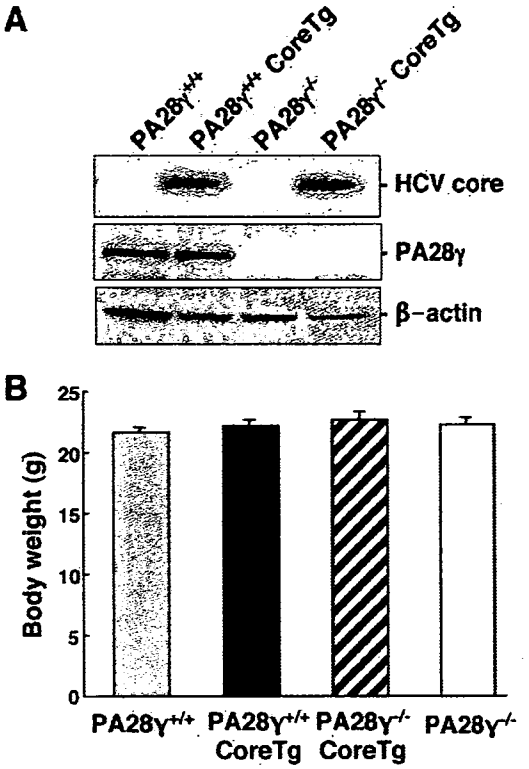

FIG. 1. Characterization of HCV core gene-transgenic mice deficient in the PA28γ gene. (A) Expression of the HCV core protein and PA28γ in the livers of PA28γ$^{+/+}$, PA28γ$^{+/+}$CoreTg, PA28γ$^{-/-}$, and PA28γ$^{-/-}$CoreTg mice. Lysates obtained from liver tissues of the mice (100 μg protein/lane) were subjected to sodium dodecyl sulfate-polyacrylamide gel electrophoresis and immunoblotting using antibodies to the HCV core protein, PA28γ, and β-actin. (B) Body weights of the mice. Body weights of 2-month-old mice were measured (n = 7 in each group). There were no statistically significant differences in body weights among the mice ($P > 0.05$).

Reporter assay for TNF-α promoter activity. The promoter region of the TNF-α gene (located from residues −1260 to +140) was amplified from mouse genomic DNA and was then introduced into the KpnI and BglII sites of pGL3-Basic (Promega, Madison, WI) (25). The resulting plasmid was designated as pGL3-tnf-aPro. The gene encoding the HCV core protein was amplified from HCV strain J1 (genotype 1b) and cloned into pCAG-GS (1, 38). To avoid contamination with endotoxin from *Escherichia coli*, the plasmid DNA was purified by using an EndoFree Plasmid Maxi kit (QIAGEN). The total amount of transfected DNA was normalized by the addition of empty plasmids. Plasmid vector was transfected into hepatoma cell lines by lipofection using Lipofectamine 2000 (Invitrogen). Cells were harvested at 24 h posttransfection. Luciferase activity was determined by using the Dual-Luciferase Reporter Assay system (Promega). Firefly luciferase activity was normalized to coexpressed *Renilla* luciferase activity. The amount of firefly luciferase activity was presented as the increase (n-fold) relative to the value for the sample lacking the HCV core protein, which was taken to be 1.0. PA28γ-knockdown cell lines were established by using pSilencer 2.1 U6 Hygro (Ambion) according to the manufacturer's protocol.

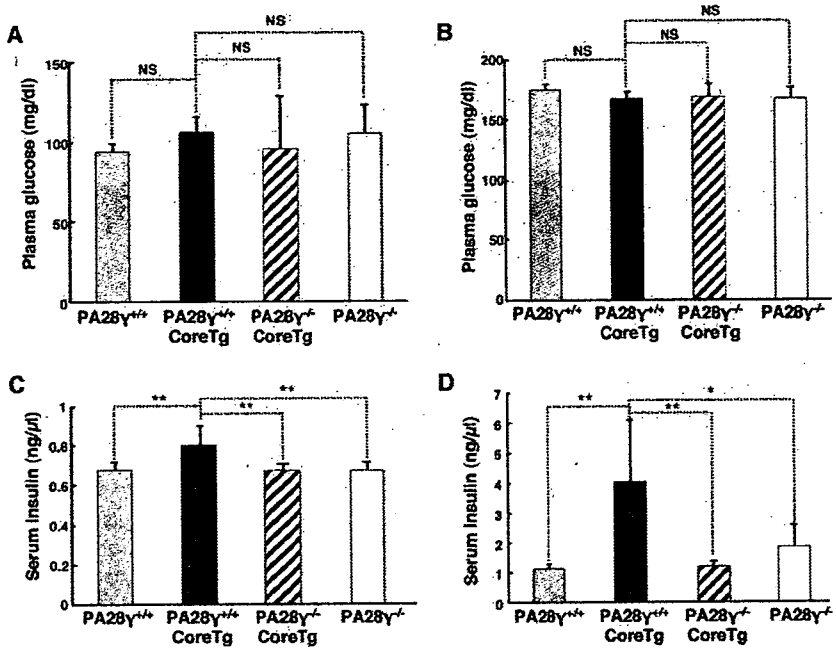

FIG. 2. Knockout of the PA28γ gene inhibited the hyperinsulinemia induced by HCV core protein. Plasma glucose levels of PA28γ$^{+/+}$, PA28γ$^{+/+}$CoreTg, PA28γ$^{-/-}$CoreTg, and PA28γ$^{-/-}$ mice under fasting (A) or fed (B) conditions (n = 7 in each group) are shown. Serum insulin levels in fasting (C) or fed (D) mice (n = 7 in each group) are also shown. Values are represented as means ± standard deviations. $*P < 0.05$; $**P < 0.01$. NS, not statistically significant.

Statistical analysis. The results are presented as means ± standard deviations. The significance of the differences was determined by Student's t test. P values of <0.05 were considered statistically significant.

RESULTS

HCV core gene-transgenic mice deficient in the PA28γ gene. To investigate the role of PA28γ in the development of insulin resistance in HCV core gene-transgenic (PA28γ$^{+/+}$CoreTg) mice, we generated HCV core gene-transgenic mice deficient in the PA28γ gene (PA28γ$^{-/-}$CoreTg). A PA28γ$^{+/+}$CoreTg mouse expressing an amount of PA28γ equal to that of its normal littermates (Fig. 1A) was crossbred with a PA28γ$^{-/-}$ mouse to generate a PA28γ$^{+/-}$ CoreTg mouse. PA28γ$^{+/-}$ CoreTg mice were bred with each other, and a PA28γ$^{-/-}$ CoreTg mouse was selected by PCR. The HCV core protein was expressed in PA28γ$^{+/+}$CoreTg and PA28γ$^{-/-}$CoreTg

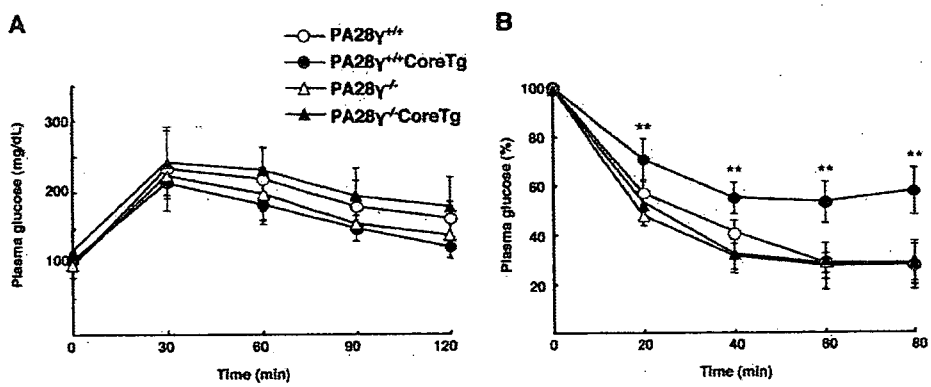

FIG. 3. Knockout of the PA28γ gene inhibits the insulin resistance induced by the HCV core protein. (A) Glucose tolerance test. D-Glucose was intraperitoneally administered to mice fasted for more than 16 h at 1 g/kg of body weight. Plasma glucose levels were estimated at the indicated times (n = 5 in each group). There were no significant differences in glucose levels among the mice ($P > 0.05$). (B) Insulin tolerance test. Human insulin (2 units/kg body weight) was intraperitoneally administered to the mice, and the plasma glucose levels were estimated at the indicated times. Values were normalized to the baseline glucose concentration at the time of insulin administration (n = 5 in each group). The values for the PA28γ$^{+/+}$ (open circles), PA28γ$^{+/+}$CoreTg (closed circles), PA28γ$^{-/-}$ (open triangles), and PA28γ$^{-/-}$CoreTg (closed triangles) mice are represented as means and ± standard deviations. Significant differences in insulin sensitivity ($P < 0.01$) in PA28γ$^{+/+}$CoreTg mice compared to that in PA28γ$^{+/+}$, PA28γ$^{-/-}$, or PA28γ$^{-/-}$CoreTg mice are indicated by double asterisks (**). There were no significant differences among PA28γ$^{+/+}$, PA28γ$^{-/-}$, and PA28γ$^{-/-}$CoreTg mice ($P > 0.05$).

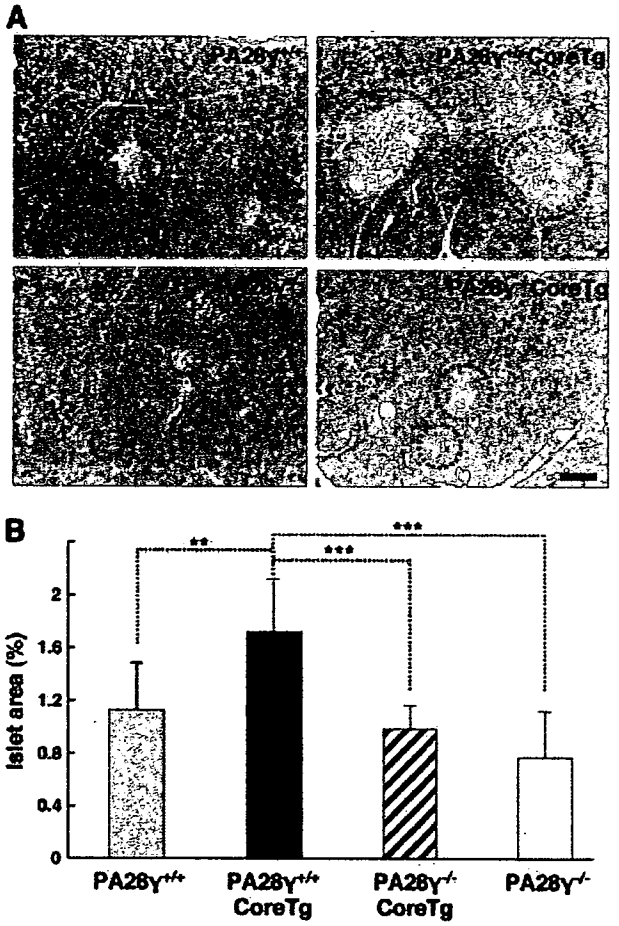

FIG. 4. PA28γ participated in the enlargement of pancreatic islets induced by the HCV core protein. (A) Histological sections prepared from pancreas tissues of PA28γ$^{+/+}$, PA28γ$^{+/+}$CoreTg, PA28γ$^{-/-}$, and PA28γ$^{-/-}$CoreTg mice were stained with hematoxylin and eosin. Dotted circles indicate pancreatic islets. (B) The area occupied by pancreatic islets was measured by computer software in three different fields of every six randomly selected sections of 10 mice per genotype and is represented as a percentage of the total pancreatic area. $**P < 0.01$; $***P < 0.001$. The scale bar indicates 100 μm.

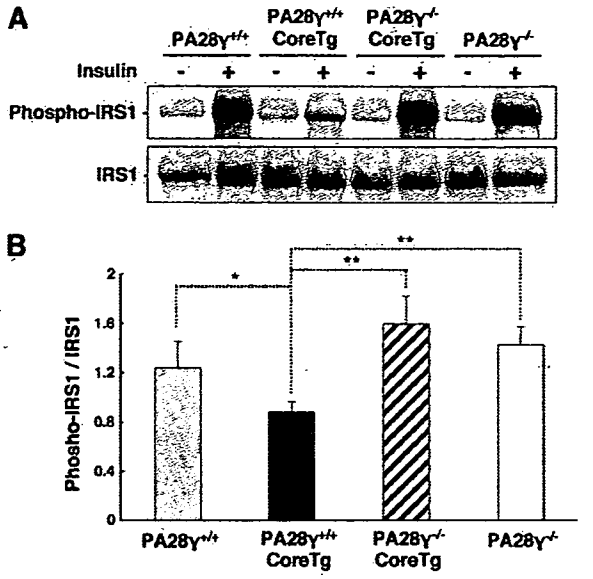

FIG. 5. PA28γ participated in the inhibition of the tyrosine phosphorylation of IRS1 induced by the HCV core protein. Liver tissues from PA28γ$^{+/+}$, PA28γ$^{+/+}$CoreTg, PA28γ$^{-/-}$, and PA28γ$^{-/-}$CoreTg mice were prepared after administration of insulin (+) or phosphate-buffered saline (−). The samples (100 μg of total protein) were examined by immunoblotting with antibodies against IRS1 and phospho-Tyr608 of mouse IRS1 (A). Phosphorylated IRS1 was estimated from the density on the immunoblotted membrane by using computer software (B) ($n = 5$ in each group). The data presented are representative of three independent experiments. $*P < 0.05$; $**P < 0.01$.

mice but not in PA28γ$^{+/+}$ (normal littermates) or PA28γ$^{-/-}$ mice. PA28γ was found at a similar level in PA28γ$^{+/+}$CoreTg and PA28γ$^{+/+}$ mice but was not present in either PA28γ$^{-/-}$ or PA28γ$^{-/-}$CoreTg mice (Fig. 1A). The expression of the HCV core protein in the livers of 2-month-old male mice was slightly higher in PA28γ$^{-/-}$CoreTg (1.36 ± 0.44 ng/mg of total protein; $n = 7$) than in PA28γ$^{+/+}$CoreTg (1.23 ± 0.22 ng/mg of total protein; $n = 7$) mice, but these values were not significantly different ($P > 0.05$). Insulin sensitivity is dependent on several conditions such as body weight, obesity, and liver steatosis (26). PA28γ$^{-/-}$ mice were slightly smaller than their normal littermates (PA28γ$^{+/+}$) at more than 3 months old, as described previously (36), but this was not significantly different in 2-month-old mice (Fig. 1B). PA28γ$^{+/+}$CoreTg mice exhibited severe hepatic steatosis from 4 months of age (35). To avoid the influence of hepatic steatosis and body weight on the examination of insulin resistance, 2-month-old mice were used in this study. Figure 1B shows the body weights of 2-month-old mice. There were no significant differences in body weight among PA28γ$^{+/+}$CoreTg, PA28γ$^{-/-}$CoreTg, PA28γ$^{-/-}$, and PA28γ$^{+/+}$ mice. Steatosis was not detected in the livers of the 2-month-old mice (data not shown).

PA28γ is involved in the development of hyperinsulinemia and insulin resistance in PA28γ$^{+/+}$CoreTg mice. In our previous study, we found a significant difference in serum insulin levels, but not in plasma glucose levels, between PA28γ$^{+/+}$ CoreTg mice and normal littermates (47). To determine the involvement of PA28γ in the development of insulin resistance in PA28γ$^{+/+}$CoreTg mice, we examined here the plasma glucose and insulin levels in the mice under fasting and fed conditions. Although no significant difference in plasma glucose levels was observed in the mice under either fasting (Fig. 2A) or fed (Fig. 2B) conditions, serum insulin levels were significantly higher in PA28γ$^{+/+}$CoreTg mice than in PA28γ$^{+/+}$ mice under both conditions (Fig. 2C and D), as described previously (47). In contrast, the serum insulin concentration in PA28γ$^{-/-}$CoreTg mice was recovered to a normal level similar to that of PA28γ$^{+/+}$ and PA28γ$^{-/-}$ mice under either fasting (Fig. 2C) or fed (Fig. 2D) conditions.

To determine the glucose intolerance among the mice, glucose was administered to the mice after fasting, and the plasma glucose level was then determined. There was no significant difference among the genotypes at any time point in the glucose tolerance test (Fig. 3A), suggesting that the volume of glucose was maintained at a normal level by the higher concentration of insulin in PA28γ$^{+/+}$CoreTg mice. In our previ-

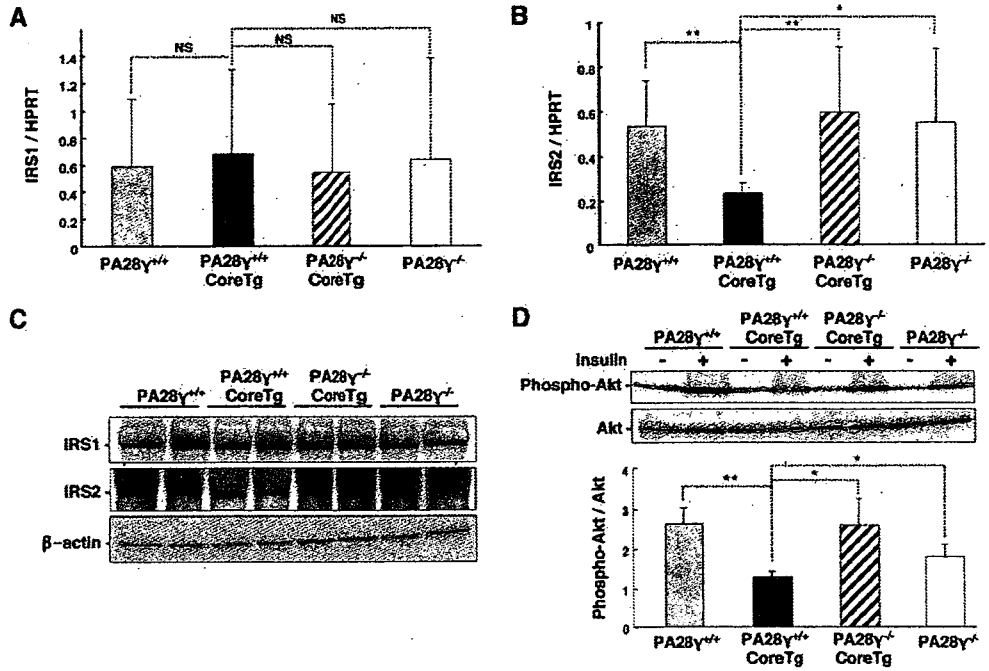

FIG. 6. PA28γ participated in the inhibition of the IRS2 expression and Akt phosphorylation induced by HCV core protein. The transcription of IRS1 (A) and IRS2 (B) was estimated by quantitative RT-PCR ($n = 5$ in each group). (C) The expression levels of IRS1 and IRS2 in the livers of the mice were determined by immunoblotting with specific antibodies. (D) Phosphorylation of Akt in the livers of the mice was examined by immunoblotting with antibodies against Akt and phosphorylated Akt. The ratio of Akt phosphorylation was determined by computer software based on the densities of phosphorylated Akt and a total amount of Akt ($n = 3$ in each group). The data presented are representative of three independent experiments. $*P < 0.05$; $**P < 0.01$. NS, not statistically significant; HPRT, hypoxanthine phosphoribosyl transferase.

ous study, the reduction in the plasma glucose concentration after insulin administration was impaired in PA28γ$^{+/+}$CoreTg mice (47). In this study, PA28γ$^{-/-}$CoreTg mice exhibited a normal insulin level comparable to those of PA28γ$^{+/+}$ and PA28γ$^{-/-}$ mice by an insulin tolerance test, in contrast to PA28γ$^{+/+}$CoreTg mice, in which a high concentration of plasma glucose was detected at all time points, as previously reported (Fig. 3B). These data suggest that hyperinsulinemia was induced in PA28γ$^{+/+}$CoreTg mice to compensate for insulin resistance and retain a physiological level of plasma glucose and that PA28γ participates in the development of hyperinsulinemia and insulin resistance in PA28γ$^{+/+}$CoreTg mice.

Morphology of pancreatic islets. Hyperinsulinemia and insulin resistance are expected to enlarge the pancreatic islet mass due to the overexpression of insulin. Our previous report showed the enlargement of the pancreatic islets in PA28γ$^{+/+}$ CoreTg mice. To clarify whether a knockout of the PA28γ gene restores the enlarged pancreatic islets to their normal size, the morphology of the pancreatic islets of the mice was evaluated by histologic examination (Fig. 4A). The relative islet area in the pancreatic cells of the PA28γ$^{-/-}$CoreTg mice was smaller than that of PA28γ$^{+/+}$CoreTg mice and comparable to that of PA28γ$^{+/+}$ and PA28γ$^{-/-}$ mice (Fig. 4B). Infiltration of inflammatory cells within or surrounding the islets was not found in all genotypes of mice. These results suggest that PA28γ also participates in the enlargement of pancreatic islets induced in PA28γ$^{+/+}$CoreTg mice.

PA28γ impairs the insulin-signaling pathway through the suppression of both tyrosine phosphorylation of IRS1 and expression of IRS2. Insulin binds to insulin receptors, resulting in the activation of downstream signaling (26). The activated insulin receptors phosphorylate themselves, IRS1, and IRS2. Phosphorylated IRS1 and IRS2 can activate phosphatidylinositol 3 (PI3)-kinase signaling, leading to the activation of glucose metabolism and cell growth. Our previous report showed that tyrosine phosphorylation of IRS1 is suppressed in the livers of PA28γ$^{+/+}$CoreTg mice and that the administration of anti-TNF-α antibody restores insulin sensitivity (47). We examined whether a knockout of the PA28γ gene could restore the tyrosine phosphorylation of IRS1. Tyrosine phosphorylation of IRS1 was suppressed in the livers of PA28γ$^{+/+}$ CoreTg mice in response to insulin stimulation, whereas it was recovered in PA28γ$^{-/-}$CoreTg mice to levels comparable to those in PA28γ$^{+/+}$and PA28γ$^{-/-}$ mice (Fig. 5).

Chronic hyperinsulinemia downregulates the expression of IRS2, which is one of the essential components of the insulin-signaling pathway in the liver (46). However, in our previous study, we showed that there was no significant difference in the phosphorylation of IRS2 between PA28γ$^{+/+}$CoreTg mice and their normal littermates (47). To gain more insight into the mechanisms of regulation of IRS expression, we determined the transcription and translation of IRS1 and IRS2 in the livers of the mice by real-time PCR and Western blotting, respectively. Although there was no significant difference in IRS1 expression at either the transcriptional or translational level among the mice

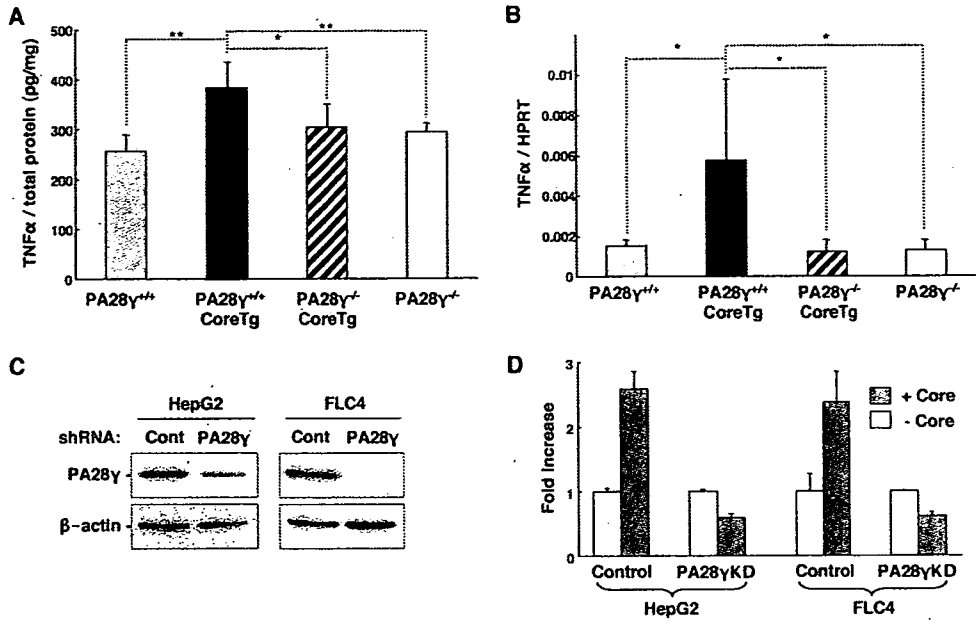

FIG. 7. PA28γ was required for activation of the TNF-α promoter by the HCV core protein. (A) Expression of TNF-α in the livers of mice was determined by ELISA (n = 5 in each group). (B) TNF-α mRNA in the livers of mice was examined by quantitative RT-PCR (n = 5 in each group). (C) Knockdown of the expression of PA28γ in the HepG2 and FLC-4 cell lines by the introduction of a plasmid encoding a short hairpin RNA (shRNA) targeted to the PA28γ gene. The expression levels of PA28γ and β-actin were determined by immunoblotting with specific antibodies. (D) Promoter activity of TNF-α in the presence or absence of the HCV core protein was determined by luciferase assay in the PA28γ-knockdown and control cell lines. The data presented are representative of three independent experiments. HPRT, hypoxanthine phosphoribosyl transferase.

(Fig. 6A and C), the expression of IRS2 was clearly impaired in PA28γ$^{+/+}$CoreTg mice at both the transcriptional and translational levels compared with that in other mice (Fig. 6B and C). The serine/threonine protein kinase Akt is phosphorylated by phosphoinositide-dependent kinase 1 (PDK1) under the activated condition of IRS family proteins (26). The insulin-induced phosphorylation of Akt was suppressed in the livers of PA28γ$^{+/+}$ CoreTg mice but not in those of PA28γ$^{+/+}$, PA28γ$^{-/-}$, or PA28γ$^{-/-}$CoreTg mice (Fig. 6D). These results suggest that the expression of the HCV core protein in the livers of mice in the presence of PA28γ impairs the insulin-signaling pathway through the suppression of both the tyrosine phosphorylation of IRS1 and the expression of IRS2.

PA28γ is required for activation of the TNF-α promoter by HCV core protein. TNF-α is an adipokine (54) and suppresses the signaling pathway of IRS1 and IRS2 (14, 42). Several reports suggested that the serum TNF-α level is higher in HCV patients than in healthy individuals (19, 37). Elevations of TNF-α levels have also been demonstrated in the livers of PA28γ$^{+/+}$CoreTg mice (47). To determine the involvement of PA28γ in the enhancement of TNF-α expression, the expression of TNF-α in the livers of each genotype was determined by ELISA and real-time PCR (Fig. 7A and B). Transcription and translation of TNF-α were increased in the livers of PA28γ$^{+/+}$ CoreTg mice but were restored in the livers of PA28γ$^{-/-}$ CoreTg mice to levels comparable to those of PA28γ$^{+/+}$ and PA28γ$^{-/-}$ mice. To determine the effect of PA28γ expression on the promoter activity of TNF-α in human liver cells, PA28γ-knockdown human hepatoma cell lines HepG2 and FLC4 were established by the introduction of a plasmid encoding a short hairpin RNA targeting the PA28γ gene in the cell lines. The expression of PA28γ was clearly suppressed in the cell lines (Fig. 7C). The expression of HCV core protein in the hepatoma cell lines potentiated TNF-α promoter activity, whereas the promoter activation by the HCV core protein was suppressed in the PA28γ-knockdown cell lines (Fig. 7D). These results suggest that PA28γ is required for the activation of the TNF-α promoter induced by the expression of the HCV core protein in human hepatoma cell lines.

DISCUSSION

HCV infection has a close association with type 2 diabetes, which is a polygenic disease with a pathophysiology that includes a defect in insulin secretion, increased hepatic glucose production, and resistance to the action of insulin (2, 8, 18). Insulin binds to insulin receptors, which exhibit tyrosine kinase activity, leading to the autophosphorylation and phosphorylation of IRS (56). Tyrosine phosphorylation in IRS proteins leads to the interaction between IRS proteins and the regulatory subunit p85 of PI3-kinase, which enhances glucose uptake and inhibits lypolysis (21). Activated PI3-kinase phosphorylates phosphatidylinositol 4,5-biphosphate to produce phosphatidylinositol 3,4,5-triphosphate, which contributes to the activation of PDK1 (55). Activated PDK1 phosphorylates downstream substrates including Akt and other kinases (55). A diabetic phenotype that included insulin resistance was found in IRS2-knockout mice with normal growth (57), although a